

Energy-Efficient Resource Allocation in OFDMA Systems with Hybrid Energy Harvesting Base Station

Derrick Wing Kwan Ng*, Ernest S. Lo[†], and Robert Schober*

*Institute for Digital Communications, Universität Erlangen-Nürnberg, Germany

[†]Centre Tecnològic de Telecomunicacions de Catalunya - Hong Kong (CTTC-HK)

Email: kwan@int.de, ernest.lo@cttc.hk, schober@int.de

Abstract

We study resource allocation algorithm design for energy-efficient communication in an orthogonal frequency division multiple access (OFDMA) downlink network with hybrid energy harvesting base station (BS). Specifically, an energy harvester and a constant energy source driven by a non-renewable resource are used for supplying the energy required for system operation. We first consider a deterministic *offline* system setting. In particular, assuming availability of non-causal knowledge about energy arrivals and channel gains, an *offline* resource allocation problem is formulated as a non-convex optimization problem over a finite horizon taking into account the circuit energy consumption, a finite energy storage capacity, and a minimum required data rate. We transform this non-convex optimization problem into a convex optimization problem by applying time-sharing and exploiting the properties of non-linear fractional programming which results in an efficient asymptotically *optimal offline* iterative resource allocation algorithm for a sufficiently large number of subcarriers. In each iteration, the transformed problem is solved by using Lagrange dual decomposition. The obtained resource allocation policy maximizes the weighted energy efficiency of data transmission (weighted bit/Joule delivered to the receiver). Subsequently, we focus on *online* algorithm design. A conventional stochastic dynamic programming approach is employed to obtain the *optimal online* resource allocation algorithm which entails a prohibitively high complexity. To strike a balance between system performance and computational complexity, we propose a low complexity *suboptimal online iterative algorithm* which is motivated by the *offline* algorithm. Simulation results illustrate that the proposed suboptimal online iterative resource allocation algorithm does not only converge in a small number of iterations, but also achieves a close-to-optimal system energy efficiency by utilizing only causal channel state and energy arrival information.

Index Terms

Energy harvesting, green communication, non-convex optimization, resource allocation.

This paper has been presented in part at the IEEE Global Communications Conference (Globecom 2012), Anaheim, California, USA.

arXiv:1302.4721v1 [cs.IT] 19 Feb 2013

I. INTRODUCTION

Orthogonal frequency division multiple access (OFDMA) is a viable multiple access scheme for spectrally efficient communication systems due to its flexibility in resource allocation and ability to exploit multiuser diversity [1], [2]. Specifically, OFDMA converts a wideband channel into a number of orthogonal narrowband subcarrier channels and multiplexes the data of multiple users on different subcarriers. In a downlink OFDMA system, the maximum system throughput can be achieved by selecting the best user on each subcarrier and adapting the transmit power over all subcarriers using water-filling. On the other hand, the increasing interest in high data rate services such as video conferencing and online high definition video streaming has led to a high demand for energy. This trend has significant financial implications for service providers due to the rapidly increasing cost of energy. Recently, driven by environmental concerns, green communication has received considerable interest from both industry and academia [3]-[6]. In fact, the cellular networks consume world-wide approximately 60 billion kWh per year. In particular, 80% of the electricity in cellular networks is consumed by the base stations (BSs) which produce over a hundred million tons of carbon dioxide per year [6]. These figures are projected to double by the year 2020 if no further actions are taken. As a result, a tremendous number of green technologies/methods have been proposed in the literature for maximizing the energy efficiency (bit-per-Joule) of wireless communication systems [7]-[10]. In [7], a closed-form power allocation solution was derived for maximizing the energy efficiency of a point-to-point single carrier system with a minimum average throughput requirement. In [8]-[10], energy efficiency has been studied in cellular multi-carrier multi-user systems for both uplink and downlink communications. Specifically, in [8]-[10], the existence of a unique global maximum for the energy efficiency was proven for different systems and can be achieved by corresponding resource allocation algorithms. On the other hand, there have been recent research efforts to enhance the system energy efficiency by using multiple antennas [11]-[13]. In [11] and [12], power loading algorithms were designed to maximize the energy efficiency of systems with collocated and distributed antennas, respectively. In [13], the authors studied the energy efficiency of cellular networks with a large number of transmit antennas in OFDMA systems. Yet, [7]-[13] require the availability of an ideal power supply such that a large amount of energy can be continuously used for system operations whenever needed. In practice, BSs may not be connected to the power grid, especially in developing countries. Thus, the assumption of a continuous energy supply made in [7]-[13] is overly optimistic in this case. Although these BSs can be possibly powered by diesel generators [14], the inefficiency of diesel fuel power generators and high transportation costs of diesel fuel are obstacles for the provision of wireless services in remote areas [15]. In such situations, energy harvesting is particularly appealing since

BSs can harvest energy from natural renewable energy sources such as solar, wind, and geothermal heat, thereby reducing substantially the operating costs of the service providers. As a result, wireless networks with energy harvesting BSs are not only envisioned to be energy-efficient in providing ubiquitous service coverage, but also to be self-sustained.

The introduction of energy harvesting capabilities for BSs poses many interesting new challenges for resource allocation algorithm design due to the time varying availability of the energy generated from renewable energy sources. In [16] and [17], optimal packet scheduling and power allocation algorithms were proposed for energy harvesting systems for minimization of the transmission completion time, respectively. In [18] and [19], the authors proposed optimal power control time sequences for maximizing the throughput by a deadline with a single energy harvester. However, these works assumed a point-to-point narrowband communication system and the obtained results may not be applicable to the case of wideband multi-user systems. In [20]-[22], different optimal packet scheduling algorithms were proposed for additive white Gaussian noise (AWGN) broadcast channels for a set of preselected users. However, wireless communication channels are not only impaired by AWGN but also degraded by multi-path fading. In addition, dynamic user selection is usually performed to enhance the system performance. On the other hand, although the amount of renewable energy is potentially unlimited, the intermittent nature of energy generated by a natural energy source results in a highly random energy availability at the BS. For example, solar energy and wind energy are varying significantly over time due to weather and climate conditions. In other words, a BS powered solely by an energy harvester may not be able to maintain a stable operation and to guarantee a certain quality of service (QoS). Therefore, a hybrid energy harvesting system design, which uses different energy sources in a complementary manner, is preferable in practice for providing uninterrupted service [23], [24]. However, the results in the literature, e.g. [7]-[22], are only valid for systems with a single energy source and are not applicable to communication networks employing hybrid energy harvesting BSs.

In this paper, we address the above issues and focus on resource allocation algorithm design for hybrid energy harvesting BSs. In Section II, we introduce the adopted OFDMA channel model and hybrid energy source model. In Section III, we formulate offline resource allocation as an optimization problem by assuming non-causal knowledge of the channel gains and energy arrivals at the BS. The optimization problem is solved via fractional programming and Lagrange dual decomposition which leads to an efficient iterative resource allocation algorithm. The derived offline solution serves as a building block for the design of a practical close-to-optimal online resource allocation algorithm in Section IV which requires only causal knowledge of the channel gains and energy arrivals. In Section V, we show that the proposed suboptimal algorithm does not only have a fast convergence, but also

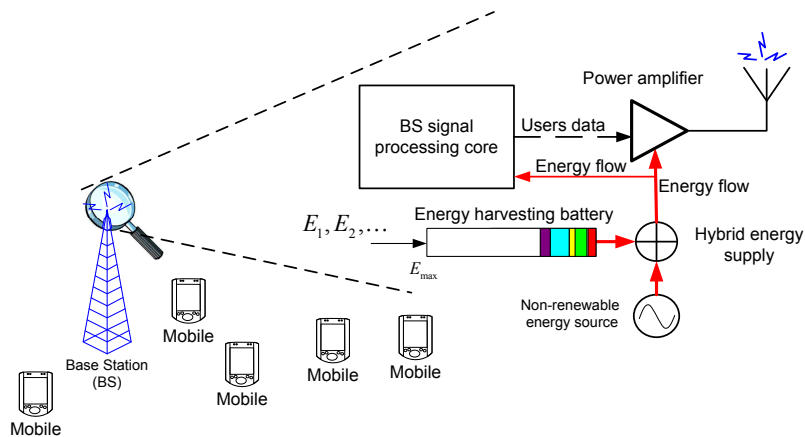


Fig. 1. An OFDMA system with a hybrid energy harvesting base station (BS) for signal transmission. Two energy sources are implemented in the system, i.e., a renewable energy harvesting source and a non-renewable energy source.

achieves a close-to-optimal performance.

II. OFDMA SYSTEM MODEL

A. Notation

A complex Gaussian random variable with mean μ and variance σ^2 is denoted by $\mathcal{CN}(\mu, \sigma^2)$, and \sim means “distributed as”. $[x]^+ = \max\{0, x\}$. $[x]_b^a = a$, if $x > a$, $[x]_b^a = x$, if $b \leq x \leq a$, $[x]_b^a = b$, if $b > x$. $\mathcal{E}_x\{\cdot\}$ denotes statistical expectation with respect to (w.r.t.) random variable \mathbf{x} .

B. OFDMA Channel Model

We consider an OFDMA network which consists of a BS and K mobile users. All transceivers are equipped with a single antenna, cf. Figure 1. The total bandwidth of the system is \mathcal{B} Hertz and there are n_F subcarriers. The transmission time is T seconds. We assume that the BS adapts the resource allocation policy (i.e., the power allocation and subcarrier allocation policies) L times for a given period T . The optimal value of L and the time instant of each adaption will be provided in the next section. The downlink symbol received at user $k \in \{1, \dots, K\}$ from the BS on subcarrier $i \in \{1, \dots, n_F\}$ at time instant¹ t , $0 \leq t \leq T$, is given by

$$y_{i,k}(t) = \sqrt{P_{i,k}(t)g_k(t)H_{i,k}(t)}x_{i,k}(t) + z_{i,k}(t), \quad (1)$$

where $x_{i,k}(t)$ is the symbol transmitted from the BS to user k on subcarrier i at time t . $P_{i,k}(t)$ is the transmit power for the link between the BS and user k on subcarrier i . $H_{i,k}(t)$ is the small scale

¹In practical systems, the length of the cyclic prefix of an orthogonal frequency-division multiplexing (OFDM) symbol is chosen to be larger than the root mean square delay spread of the channel. Nevertheless, the channel gains from one subcarrier to the next may change considerably. Therefore, we use a discrete model for the frequency domain. On the other hand, the coherence time for a low mobility user is about 200 ms and an OFDM symbol in Long-Term-Evolution (LTE) systems has a length of 71.3 μ s. Thus, during a transmission time T much longer than the coherence time, e.g., $T \gg 200$ ms, a few thousands of OFDM symbols are transmitted. Therefore, we use a continuous time domain signal model for representing the time variation of the signals.

fading coefficient between the BS and user k on subcarrier i at time t . $g_k(t)$ represents the joint effect of path loss and shadowing between the BS and user k at time t . $z_{i,k}(t)$ is the AWGN in subcarrier i at user k with distribution $\mathcal{CN}(0, N_0)$, where N_0 is the noise power spectral density.

C. Models for Time Varying Fading and Energy Sources

In the BS, there are two energy sources for supplying the energy required for system operation, i.e., an energy harvester and a constant energy source driven by a non-renewable resource, cf. Figure 1. In practice, the model for the energy harvester depends on its specific implementation. For instance, both solar panel and wind turbine-generator are able to generate renewable energy for communication purposes. Yet, the energy harvesting characteristics (i.e., energy arrival dynamics and the amount of energy being harvested) are different in both cases. In order to provide a general model for energy harvesting communication systems, we do not assume a particular type of energy harvester. Instead, we model the energy output characteristic of the energy harvester as a stochastic process in order to isolate the considered problem from specific implementation assumptions. In particular, we adopt a similar system model as in [19] for modeling the time varying nature of the communication channels and the random energy arrival behavior in the energy harvester. We assume that the energy arrival times in the energy harvester are modeled as a Poisson counting process with rate λ_E . Therefore, the energy arrivals occur in a countable number of time instants, which are indexed as $\{t_1^E, t_2^E, \dots\}$. The inter-occurrence time between two consecutive energy arrivals, i.e., $t_b^E - t_{b-1}^E, b \in \{1, 2, \dots\}$, is exponentially distributed with mean $1/\lambda_E$. Besides, E_b units of energy arrive (to be harvested) at the BS at time t_b^E . On the other hand, a block fading communication channel model is considered, cf. [19], [25], [26]. Without loss of generality, we denote the time instants where the fading level changes as $\{t_1^F, t_2^F, \dots\}$. We note that the fading level in $0 < t \leq t_1^F$ is constant but changes² to an independent value in the next time interval of fading block, $t_1^F < t \leq t_2^F$, and so on. The length of each fading block is approximately equal to the coherence time of the channel³, cf. Figure 2. The incoming energy is collected by an energy harvester and is buffered in the battery before it is used for data transmission. On the other hand, we assume that E_0 units of energy arrive(/are available) in the

²In the paper, the changes in channel gain refer to the changes in $H_{i,k}(t)$. In fact, $g_k(t)$ is assumed to be a constant over time T . The coherence time of the shadowing and path loss is proportional to the coherence distance. For instance, the coherence distance in a suburban area is around 100-200 m and tens of meters in an urban area [27]. Assuming a coherence distance of 100 m, this results in a coherence time of about 120 seconds at 3 km/h (pedestrian speed). Then, the coherence time of the multipath fading is an order of magnitude smaller than the coherence time of the shadowing.

³In the paper, we assume that all users have a similar velocity such that their channels have a similar coherence time. Yet, our model can be generalized to different coherence times for different users, at the expense of a more involved notation.

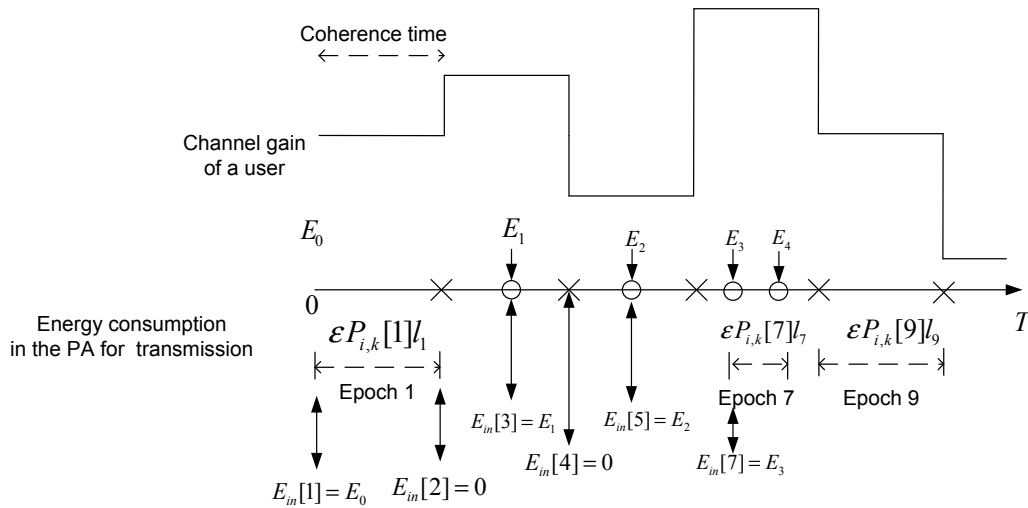


Fig. 2. An illustration of epoch and $E_{in}[\cdot]$ in (17) for different events at different arrival times. Fading changes and energies are harvested at time instants denoted by \times and \circ , respectively.

battery at $t_0^E = 0$ and the maximum amount of energy storage in the battery is denoted by E_{\max} . In the following, we refer to a change of the channel gain of any user or the energy level in the battery as an *event* and the time interval between two consecutive events as an *epoch*. Specifically, *epoch* l , $l \in \{1, 2, \dots\}$, is defined as the time interval $[t_{l-1}, t_l)$, where t_{l-1} and t_l are the time instants at which successive events happen, cf. Figure 2.

Remark 1: We note that the major assumption made in the modelling of the problem is the stationarity and ergodicity of the fading and the energy arrival random processes. In fact, the assumption of particular distributions for the changes in fading gains, time of changes in fading gains, and/or energy arrival times do not change the structure of the algorithms presented in the paper as long as the corresponding distributions are known at the BS. This knowledge can be obtained via long term measurements. The assumption of a Poisson counting process for the energy arrivals is made for illustration of the countability of the incoming energy arrivals.

In the considered model, the transmitter can draw the energy required for signal transmission and signal processing from both the battery⁴ and the traditional energy source. In particular, the instantaneous total radio frequency (RF) transmit power of the power amplifier (PA) for user k in subcarrier i at time instant t can be modeled as

$$P_{i,k}(t) = P_{i,k}^E(t) + P_{i,k}^N(t), \quad \forall i, k, 0 \leq t \leq T, \quad (2)$$

where $P_{i,k}^E(t)$ and $P_{i,k}^N(t)$ are the portions of the instantaneous transmitted power taken from the energy harvester and the non-renewable energy source for user k in subcarrier i at time instant t , respectively. Furthermore, we model the energy consumption required for signal processing as

$$\int_0^t \left(P_C^E(u) + P_C^N(u) \right) du = P_C t, \quad 0 \leq t \leq T, \quad (3)$$

⁴Note that the term “battery” is used interchangeably with the term “energy harvester” in the paper.

where $P_C^E(t)$ and $P_C^N(t)$ are the portions of the instantaneous power required for signal processing drawn from the energy harvester and the non-renewable energy source, respectively. P_C is the required constant signal processing power at each time instant and includes the power dissipation in the mixer, transmit filters, frequency synthesizer, and digital-to-analog converter (DAC), etc.

Since two energy sources are implemented at the BS, we have to consider the physical constraints imposed by both energy sources, which are described in the following.

1) *Energy Harvesting Source*: There are two inherent constraints on the energy harvester:

$$\text{C1: } \underbrace{\sum_{i=1}^{n_F} \sum_{k=1}^K \int_0^{t_b^E - \delta} \varepsilon s_{i,k}(u) P_{i,k}^E(u) du}_{\text{Energy from energy harvester used in PA}} + \int_0^{t_b^E - \delta} P_C^E(u) du \leq \sum_{j=0}^{b-1} E_j, \forall b \in \{1, 2, \dots\}, \quad (4)$$

$$\text{C2: } \sum_{j=0}^{d(t)} E_j - \sum_{i=1}^{n_F} \sum_{k=1}^K \int_0^t \varepsilon s_{i,k}(u) P_{i,k}^E(u) du - \int_0^t P_C^E(u) du \leq E_{\max}, \quad 0 \leq t \leq T, \quad (5)$$

where $\delta \rightarrow 0$ is an infinitesimal positive constant for modeling purpose⁵, $d(t) = \arg \max_a \{t_a^E : t_a^E \leq t\}$, $s_{i,k}(t) \in \{0, 1\}$ is the binary subcarrier allocation indicator at time t , and $\varepsilon \geq 1$ is constant which accounts for the inefficiency of the PA. For example, when $\varepsilon = 10$, 100 Watts of power are consumed in the PA for every 10 Watts of power radiated in the RF. In other words, the power efficiency is $\frac{1}{\varepsilon} = \frac{1}{10} = 10\%$. Constraint C1 implies that in every time instant, if the BS draws energy from the energy harvester to cover the energies required at the PA and for signal processing, it is constrained to use at most the amount of stored energy currently available (causality), even though more energy may possibly arrive in the future. Constraint C2 states that the energy level in the battery never exceeds E_{\max} in order to prevent energy overflow in(/overcharging to) the battery. In practice, energy overflow may occur if the BS is equipped with a small capacity battery.

2) *Non-renewable Energy Source*: In each time instant, a maximum power of P_N Watts can be provided by the non-renewable energy source to the BS. In other words, a maximum of $P_N t$ Joules of energy can be drawn from the non-renewable source from time zero up to time t . As a result, we have the following constraint on drawing power/energy from the non-renewable energy source at any time instant:

$$\text{C3: } \underbrace{\sum_{i=1}^{n_F} \sum_{k=1}^K \varepsilon s_{i,k}(t) P_{i,k}^N(t)}_{\text{Power from non-renewable source used in PA}} + P_C^N(t) \leq P_N, \quad 0 \leq t \leq T. \quad (6)$$

⁵The integral in equation (4) is defined over a half-open interval in $[0, t_b^E)$. As a result, the variable δ is used to account for an infinitesimal gap between the upper limit of integration and the boundary t_b^E .

III. OFFLINE RESOURCE ALLOCATION AND SCHEDULING DESIGN

In this section, we design an offline resource allocation algorithm by assuming the availability of non-causal knowledge of energy arrivals and channel gains.

A. Channel Capacity and Energy Efficiency

In this subsection, we define the adopted system performance measure. At the BS, the data buffers for the users are assumed to be always full and there are no empty scheduling slots due to an insufficient number of data packets at the buffers. Given perfect channel state information (CSI) at the receiver, the channel capacity⁶ between the BS and user k on subcarrier i over a transmission period of T second(s) with subcarrier bandwidth $W = \frac{B}{n_F}$ is given by

$$C_{i,k} = \int_0^T s_{i,k}(t) W \log_2 \left(1 + P_{i,k}(t) \Gamma_{i,k}(t) \right) dt \quad \text{where} \quad \Gamma_{i,k}(t) = \frac{g_k(t) |H_{i,k}(t)|^2}{N_0 W}. \quad (7)$$

The *weighted total system capacity* is defined as the weighted sum of the total number of bits successfully delivered to the K mobile users over a duration of T seconds and is given by

$$U(\mathcal{P}, \mathcal{S}) = \sum_{k=1}^K \alpha_k \sum_{i=1}^{n_F} C_{i,k}, \quad (8)$$

where $\mathcal{P} = \{P_{i,k}^E(t), P_{i,k}^N(t), P_C^E(t), P_C^N(t), \forall i, k, 0 \leq t \leq T\}$ and $\mathcal{S} = \{s_{i,k}(t), \forall i, k, 0 \leq t \leq T\}$ are the power and subcarrier allocation policies, respectively. $0 < \alpha_k \leq 1$ is a positive constant provided by upper layers, which allows the BS to give different priorities to different users and to enforce certain notions of fairness. On the other hand, we take into account the total energy consumption of the system by including it in the optimization objective function. For this purpose, we model the *weighted energy dissipation* in the system as the sum of two dynamic terms

$$U_{TP}(\mathcal{P}, \mathcal{S}) = \int_0^T \left(\phi P_C^E(t) + P_C^N(t) \right) dt + \sum_{k=1}^K \sum_{i=1}^{n_F} \int_0^T s_{i,k}(t) \varepsilon \left(\phi P_{i,k}^E(t) + P_{i,k}^N(t) \right) dt, \quad (9)$$

where ϕ is a positive constant imposed on the use of the harvested energy. The value of ϕ can reflect either a normalized physical cost (e.g., relative cost for maintenance/operation of both sources of energy) or a normalized virtual cost (e.g., energy usage preferences), w.r.t. the usage of the non-renewable energy source [28]. In practice, we set $0 < \phi < 1$ to encourage the BS to consume energy from the energy harvesting source. The first term and second term in (9) denote the total weighted

⁶In general, if the future CSI is not available at the BS, the randomness of the multipath fading causes resource allocation mismatches at the BS which decreases the system capacity. For instance, if only causal knowledge of multipath coefficients is available at the BS, the BS may transmit exceedingly large amounts of power at a given time instant and exhaust all the energy of the energy harvester, even though there may be much better channel conditions in the next fading block which deserve more transmission energy for improving the system energy efficiency/capacity.

energy consumptions in the signal processing unit and the PA, respectively. Hence, the *weighted energy efficiency* of the considered system over a time period of T seconds is defined as the total average number of weighted bit/Joule

$$U_{eff}(\mathcal{P}, \mathcal{S}) = \frac{U(\mathcal{P}, \mathcal{S})}{U_{TP}(\mathcal{P}, \mathcal{S})}. \quad (10)$$

B. Optimization Problem Formulation

The optimal power allocation policy, \mathcal{P}^* , and subcarrier allocation policy, \mathcal{S}^* , can be obtained by solving

$$\begin{aligned} & \max_{\mathcal{P}, \mathcal{S}} U_{eff}(\mathcal{P}, \mathcal{S}) & (11) \\ & \text{s.t.} & \text{C1, C2, C3} \\ \text{C4: } & \int_0^t (P_C^E(u) + P_C^N(u)) du = P_C t, \quad 0 \leq t \leq T, & \text{C5: } \sum_{k=1}^K \sum_{i=1}^{n_F} C_{i,k} \geq R_{\min}, \\ \text{C6: } & \sum_{i=1}^{n_F} \sum_{k=1}^K P_{i,k}(t) s_{i,k}(t) \leq P_{\max}, \quad 0 \leq t \leq T, & \text{C7: } s_{i,k}(t) = \{0, 1\}, \quad \forall i, k, 0 \leq t \leq T, \\ \text{C8: } & \sum_{k=1}^K s_{i,k}(t) \leq 1, \quad \forall i, 0 \leq t \leq T, & \text{C9: } P_{i,k}^N(t), P_{i,k}^E(t), P_C^N(t), P_C^E(t) \geq 0, \quad \forall i, k, 0 \leq t \leq T, \end{aligned}$$

where C4 ensures that the energy required for signal processing is always available⁷. C5 specifies the minimum system data rate requirement R_{\min} which acts as a QoS constraint for the system. Note that although variable R_{\min} in C5 is not an optimization variable in this paper, a balance between energy efficiency and aggregate system capacity can be struck by varying R_{\min} . C6 is a constraint on the maximum transmit power of the BS. The value of P_{\max} in C6 puts a limit on the transmit spectrum mask to control the amount of out-of-cell interference in the downlink at every time instant. Constraints C7 and C8 are imposed to guarantee that each subcarrier will be used to serve at most one user at any time instant. C9 is the non-negative constraint on the power allocation variables.

Remark 2: We note that an individual data rate requirement for each user can be incorporated into the current problem formulation by imposing the individual data rate requirements as additional constraints in the problem formulation [29], [30], i.e., C10 : $\sum_{i=1}^{n_F} C_{i,k} \geq R_{\min_k}, k \in \mathcal{D}$, where \mathcal{D} is a set of *delay sensitive* users and R_{\min_k} is a constant which specifies the minimal required data rate

⁷ In the considered system, the BS always has sufficient energy for CSI estimation despite the intermittent nature of energy generated by the energy harvester. Indeed, the BS is able to extract energy from both the traditional power supply (from the power generator) and the energy harvester. In the worst case, if the energy harvester is unable to harvest enough energy from the environment, the BS can always extract power from the traditional power supply for supporting the energy consumption of signal processing in the BS.

of user k . The resulting problem can be solved via a similar approach as used for solving the current problem formulation.

C. Transformation of the Objective Function

The optimization problem in (11) is non-convex due to the fractional form of the objective function and the combinatorial constraint C7 on the subcarrier allocation variable. We note that there is no standard approach for solving non-convex optimization problems. In order to derive an efficient power allocation algorithm for the considered problem, we introduce a transformation to handle the objective function via nonlinear fractional programming [31]. Without loss of generality, we define the maximum weighted energy efficiency q^* of the considered system as

$$q^* = \frac{U(\mathcal{P}^*, \mathcal{S}^*)}{U_{TP}(\mathcal{P}^*, \mathcal{S}^*)} = \max_{\mathcal{P}, \mathcal{S}} \frac{U(\mathcal{P}, \mathcal{S})}{U_{TP}(\mathcal{P}, \mathcal{S})}. \quad (12)$$

We are now ready to introduce the following Theorem.

Theorem 1: The maximum weighted energy efficiency q^* is achieved if and only if

$$\max_{\mathcal{P}, \mathcal{S}} U(\mathcal{P}, \mathcal{S}) - q^* U_{TP}(\mathcal{P}, \mathcal{S}) = U(\mathcal{P}^*, \mathcal{S}^*) - q^* U_{TP}(\mathcal{P}^*, \mathcal{S}^*) = 0, \quad (13)$$

for $U(\mathcal{P}, \mathcal{S}) \geq 0$ and $U_{TP}(\mathcal{P}, \mathcal{S}) > 0$.

Proof: The proof of Theorem 1 is similar to the proof in [32, Appendix A].

Theorem 1 reveals that for any objective function in fractional form, there exists an equivalent objective function in subtractive form, e.g. $U(\mathcal{P}, \mathcal{S}) - q^* U_{TP}(\mathcal{P}, \mathcal{S})$ in the considered case, which shares the same optimal resource allocation policy. As a result, we can focus on the equivalent objective function for finding the optimal offline resource allocation policy in the rest of the paper.

D. Iterative Algorithm for Energy Efficiency Maximization

In this section, an iterative algorithm (known as the Dinkelbach method [31]) is proposed for solving (11) by exploiting objective function $U(\mathcal{P}, \mathcal{S}) - q U_{TP}(\mathcal{P}, \mathcal{S})$. The proposed algorithm is summarized in Table I. Its convergence to the optimal energy efficiency is guaranteed if we are able to solve the inner problem (14) in each iteration.

Proof: Please refer to [32, Appendix B] for a proof of convergence.

As shown in Table I, in each iteration of the main loop, we solve the following optimization problem for a given parameter q :

$$\begin{aligned} & \max_{\mathcal{P}, \mathcal{S}} U(\mathcal{P}, \mathcal{S}) - q U_{TP}(\mathcal{P}, \mathcal{S}) \\ & \text{s.t. C1, C2, C3, C4, C5, C6, C7, C8, C9.} \end{aligned} \quad (14)$$

TABLE I

ITERATIVE RESOURCE ALLOCATION ALGORITHM FOR SUBOPTIMAL ONLINE AND OPTIMAL OFFLINE DESIGNS.

Algorithm 1 Iterative Algorithm for Suboptimal Online and Optimal Offline Designs

```

1: Initialize the maximum number of iterations  $I_{max}$  and the maximum tolerance  $\Delta$ 
2: Set maximum energy efficiency  $q = 0$  and iteration index  $n = 0$ 
3: repeat {Main Loop}
4:   if {Offline Problem} then
5:     Solve the inner loop problem in (14) for a given  $q$  and obtain resource allocation policies  $\{\mathcal{P}', \mathcal{S}'\}$ 
6:   else {Online Problem}
7:     Solve the inner loop problem in (40) for a given  $q$  for each event and obtain resource allocation policies  $\{\mathcal{P}', \mathcal{S}'\}$ 
8:   end if
9:   if  $U(\mathcal{P}', \mathcal{S}') - qU_{TP}(\mathcal{P}', \mathcal{S}') < \Delta$  then
10:    Convergence = true
11:    return  $\{\mathcal{P}^*, \mathcal{S}^*\} = \{\mathcal{P}', \mathcal{S}'\}$  and  $q^* = \frac{U(\mathcal{P}', \mathcal{S}')}{U_{TP}(\mathcal{P}', \mathcal{S}'')}$ 
12:   else
13:     Set  $q = \frac{U(\mathcal{P}', \mathcal{S}')}{U_{TP}(\mathcal{P}', \mathcal{S}'')}$  and  $n = n + 1$ 
14:     Convergence = false
15:   end if
16: until Convergence = true or  $n = I_{max}$ 

```

Solution of the Main Loop Problem: Although the objective function is now transformed into a subtractive form which is easier to handle, there are still two obstacles in solving the above problem. First, the equivalent problem in each iteration is a mixed combinatorial and convex optimization problem. The combinatorial nature comes from the binary constraint C7 for subcarrier allocation. To obtain an optimal solution, an exhaustive search is needed in every time instant which entails a complexity of $\mathcal{O}(K^{n_F})$ and is computationally infeasible for $K, n_F \gg 1$. Second, the optimal resource allocation policy is expected to be time varying in the considered duration of T seconds. However, it is unclear how often the BS should update the resource allocation policy which is a hurdle for designing a practical resource allocation algorithm, even for the case of offline resource allocation. In order to strike a balance between solution tractability and computational complexity, we handle the above issues in two steps. First, we follow the approach in [33] and relax $s_{i,k}(t)$ in constraint C7 to be a real value between zero and one instead of a Boolean, i.e., $0 \leq s_{i,k}(t) \leq 1$. Then, $s_{i,k}(t)$ can be interpreted as a time-sharing factor for the K users to utilize subcarrier i . For facilitating the time sharing on each subcarrier, we introduce three new variables and define them as $\tilde{P}_{i,k}^E(t) = P_{i,k}^E(t)s_{i,k}(t)$, $\tilde{P}_{i,k}^N(t) = P_{i,k}^N(t)s_{i,k}(t)$, and $\tilde{P}_{i,k}(t) = P_{i,k}(t)s_{i,k}(t)$. These variables represent the actual transmitted powers in the RF of the BS on subcarrier i for user k under the time-sharing assumption. Although

the relaxation of the subcarrier allocation constraint will generally result in a suboptimal solution, the authors in [10], [34] show that the duality gap (sub-optimality) becomes zero when the number of subcarriers is sufficiently large for any multicarrier system that satisfies time-sharing⁸. Second, we introduce the following lemma which provides valuable insight about the time varying dynamic of the optimal resource allocation policy.

Lemma 1: The optimal offline resource allocation policy⁹ maximizing the system weighted energy efficiency does not change within an epoch.

Proof: Please refer to the Appendix for a proof of Lemma 1.

As revealed by Lemma 1, the optimal resource allocation policy maximizing the weighted system energy efficiency is a constant in each epoch. Therefore, we can discretize the integrals and continuous variables in (14). In other words, the number of constraints in (14) reduce to countable quantities. Without loss of generality, we assume that the channel states change $M \geq 0$ times and energy arrives $N \geq 0$ times in the duration of $[0, T]$. Hence, we have $L = M + N$ epoch(s) for the considered duration of T seconds. Time instant T is treated as an extra fading epoch with zero channel gains for all users to terminate the process. We define the length of an epoch as $l_j = t_j - t_{j-1}$ where epoch $j \in \{1, 2, \dots, M + N\}$ is defined as the time interval $[t_{j-1}, t_j)$, cf. Figure 2. Note that t_0 is defined as $t_0 = 0$. For the sake of notational simplicity and clarity, we replace all continuous-time variables with corresponding discrete time variables, i.e., $\tilde{P}_{i,k}(t) \rightarrow \tilde{P}_{i,k}[j]$, $\tilde{P}_{i,k}^E(t) \rightarrow \tilde{P}_{i,k}^E[j]$, $\tilde{P}_{i,k}^N(t) \rightarrow \tilde{P}_{i,k}^N[j]$, $P_C^E(t) \rightarrow P_C^E[j]$, $P_C^N(t) \rightarrow P_C^N[j]$, $s_{i,k}(t) \rightarrow s_{i,k}[j]$, $H_{i,k}(t) \rightarrow H_{i,k}[j]$, $g_k(t) \rightarrow g_k[j]$, and $\Gamma_{i,k}(t) \rightarrow \Gamma_{i,k}[j]$. Then, the *weighted total system capacity* and the *weighted total energy consumption* can be re-written as

$$U(\mathcal{P}, \mathcal{S}) = \sum_{k=1}^K \alpha_k \sum_{i=1}^{n_F} \sum_{j=1}^L l_j C_{i,k}[j] \quad \text{and} \quad (15)$$

$$U_{TP}(\mathcal{P}, \mathcal{S}) = \sum_{j=1}^L l_j \left(\phi P_C^E[j] + P_C^N[j] \right) + \sum_{k=1}^K \sum_{i=1}^{n_F} \sum_{j=1}^L l_j \varepsilon \left(\phi \tilde{P}_{i,k}^E[j] + \tilde{P}_{i,k}^N[j] \right), \quad (16)$$

respectively, where $C_{i,k}[j] = s_{i,k}[j] W \log_2 \left(1 + \frac{\tilde{P}_{i,k}[j] \Gamma_{i,k}[j]}{s_{i,k}[j]} \right)$ is the channel capacity between the BS and user k on subcarrier i in epoch j . As a result, the optimization problem in (14) is transformed

⁸The proposed offline solution is asymptotically optimal when the number of subcarriers is large [10], [34]. In fact, it has been shown in [2] via simulation that the duality gap is virtually zero for only 8 subcarriers in an OFDMA system. Besides, the number of subcarriers employed in practical systems such as LTE is in the order of hundreds. In other words, the solution obtained under the relaxed time-sharing problem formulation is asymptotically optimal with respect to the original problem formulation. On the other hand, we note that although time-sharing relaxation is assumed, the solution in (24) indicates that the subcarrier allocation is still a Boolean which satisfies the binary constraint on the subcarrier allocation of the original problem.

⁹Here, ‘‘optimality’’ refers to the optimality for the problem formulation under the time-sharing assumption.

into to the following convex optimization problem:

$$\begin{aligned} & \max_{\mathcal{P}, \mathcal{S}} U(\mathcal{P}, \mathcal{S}) - qU_{TP}(\mathcal{P}, \mathcal{S}) \quad (17) \\ \text{C1: } & \sum_{i=1}^{n_F} \sum_{k=1}^K \sum_{j=1}^e l_j \varepsilon \tilde{P}_{i,k}^E[j] + \sum_{j=1}^e P_C^E[j] l_j \leq \sum_{j=1}^e E_{in}[j], \quad \forall e \in \{1, 2, \dots, M+N\}, \\ \text{C2: } & \sum_{j=1}^r E_{in}[j] - \sum_{i=1}^{n_F} \sum_{k=1}^K \sum_{j=1}^{r-1} \varepsilon l_j \tilde{P}_{i,k}^E[j] - \sum_{j=1}^{r-1} l_j P_C^E[j] \leq E_{\max}, \quad \forall r \in \{2, \dots, M+N+1\}, \\ \text{C3: } & \sum_{i=1}^{n_F} \sum_{k=1}^K l_e \varepsilon \tilde{P}_{i,k}^N[e] + l_e P_C^N[e] \leq P_N l_e, \quad \forall e, \quad \text{C4: } l_e P_C^E[e] + l_e P_C^N[e] = l_e P_C, \quad \forall e, \\ \text{C5: } & \sum_{k=1}^K \sum_{i=1}^{n_F} \sum_{j=1}^L l_j C_{i,k}[j] \geq R_{\min}, \quad \text{C6: } \sum_{i=1}^{n_F} \sum_{k=1}^K l_e \tilde{P}_{i,k}[e] \leq l_e P_{\max}, \quad \forall e, \\ \text{C7: } & 0 \leq s_{i,k}[e] \leq 1, \quad \forall e, i, k, \quad \text{C8: } \sum_{k=1}^K s_{i,k}[e] \leq 1, \quad \forall e, i, \quad \text{C9: } P_{i,k}^N[e], P_{i,k}^E[e], P_C^N[e], P_C^E[e] \geq 0, \quad \forall i, k, e, \end{aligned}$$

where $E_{in}[j]$ in C1 is defined as the energy which arrives in epoch j . Hence, $E_{in}[j] = E_a$ for some a if event j is an energy arrival and $E_{in}[j] = 0$ if event j is a channel gain change, cf. Figure 2. The transformed problem in (17) is jointly concave w.r.t. all optimization variables¹⁰, and under some mild conditions [35], solving the dual problem is equivalent to solving the primal problem.

Remark 3: Mathematically, l_e on both sides of the (in)equalities in C3, C4, and C6 in (17) can be cancelled. Nevertheless, we do think that it is desirable to keep l_e in these constraints since they preserve the physical meaning of C6; the energy consumption constraints in the system in time duration l_e .

E. Dual Problem Formulation

In this subsection, we solve transformed optimization problem (17). For this purpose, we first need the Lagrangian function of the primal problem. Upon rearranging terms, the Lagrangian can be written as

$$\begin{aligned} \mathcal{L}(\boldsymbol{\gamma}, \boldsymbol{\beta}, \rho, \boldsymbol{\mu}, \boldsymbol{\nu}, \boldsymbol{\psi}, \boldsymbol{\eta}, \mathcal{P}, \mathcal{S}) &= \sum_{j=1}^L \sum_{k=1}^K \alpha_k \sum_{i=1}^{n_F} l_j (w_k + \rho) C_{i,k}[j] - \rho R_{\min} + \sum_{j=1}^L \sum_{i=1}^{n_F} \sum_{k=1}^K \eta_{i,j} \\ &- \sum_{j=1}^L \gamma_j \left(\sum_{i=1}^{n_F} \sum_{k=1}^K \sum_{m=1}^j \varepsilon l_m \tilde{P}_{i,k}^E[m] + \sum_{m=1}^j l_m P_C^E[m] - \sum_{m=1}^j E_{in}[m] \right) - \sum_{j=1}^L \nu_j l_j (P_C^E[j] + P_C^N[j]) \end{aligned}$$

¹⁰We can follow a similar approach as in Appendix A to prove the concavity of the above problem for the considered discrete time model.

$$\begin{aligned}
& -q \left(\sum_{j=1}^L l_j \left(\phi P_C^E[j] + P_C^N[j] \right) + \sum_{k=1}^K \sum_{i=1}^{n_F} \sum_{j=1}^L l_j \varepsilon \left(\phi \tilde{P}_{i,k}^E[j] + \tilde{P}_{i,k}^N[j] \right) \right) + \sum_{j=1}^L \nu_j l_j P_C \\
& - \sum_{j=2}^{L+1} \beta_j \left(\sum_{m=1}^j E_{in}[m] - \sum_{i=1}^{n_F} \sum_{k=1}^K \sum_{m=1}^{j-1} \varepsilon l_m \tilde{P}_{i,k}^E[m] - \sum_{m=1}^{j-1} l_m P_C^E[m] - E_{\max} \right) - \sum_{j=1}^L \sum_{i=1}^{n_F} \sum_{k=1}^K \eta_{i,j} s_{i,k}[j] \\
& - \sum_{j=1}^L \mu_j \left(\sum_{i=1}^{n_F} \sum_{k=1}^K \varepsilon l_j \tilde{P}_{i,k}^N[j] + l_j P_C^N[j] - l_j P_N \right) - \sum_{j=1}^L \psi_j \left(\sum_{i=1}^{n_F} \sum_{k=1}^K l_j \tilde{P}_{i,k}[j] - l_j P_{\max} \right), \tag{18}
\end{aligned}$$

where γ is the Lagrange multiplier vector associated with causality constraint C1 on consuming energy from the energy harvester and has elements γ_j , $j \in \{1, \dots, L\}$. β is the Lagrange multiplier vector corresponding to the maximum energy level constraint C2 in the battery of the energy harvester with elements β_j where $\beta_1 = 0$. ρ is the Lagrange multiplier corresponding to the minimum data rate requirement R_{\min} in C5. μ , ν , and ψ have elements μ_j , ν_j , and ψ_j are the Lagrange multiplier vectors for constraints C3, C4, and C6, respectively. η is the Lagrange multiplier vector accounting for subcarrier usage constraint C8 with elements $\eta_{i,j}$, $i \in \{1, \dots, n_F\}$. Note that the boundary constraints C7 and C9 are absorbed into the Karush-Kuhn-Tucker (KKT) conditions when deriving the optimal solution in Section III-F.

Thus, the dual problem is given by

$$\min_{\gamma, \beta, \rho, \mu, \psi, \eta \geq 0} \max_{\mathcal{P}, \mathcal{S}} \mathcal{L}(\gamma, \beta, \rho, \mu, \nu, \psi, \eta, \mathcal{P}, \mathcal{S}). \tag{19}$$

Note that ν is not an optimization variable in (19) since C4 in (17) is an equality constraint.

F. Dual Decomposition and Subproblem Solution

By Lagrange dual decomposition, the dual problem is decomposed into two parts (nested loops): the first part (inner loop) consists of $n_F + 1$ subproblems where n_F subproblems have identical structure; the second part (outer loop) is the master dual problem. The dual problem can be solved iteratively where in each iteration the BS solves n_F subproblems (inner loop) in parallel and solves the master problem (outer loop) with the gradient method.

Each one of the n_F subproblems with identical structure is designed for one subcarrier and can be expressed as

$$\max_{\mathcal{P}, \mathcal{S}} \mathcal{L}_i(\gamma, \beta, \rho, \mu, \nu, \psi, \eta, \mathcal{P}, \mathcal{S}) \tag{20}$$

for a fixed set of Lagrange multipliers where

$$\begin{aligned}
\mathcal{L}_i(\gamma, \beta, \rho, \mu, \nu, \psi, \eta, \mathcal{P}, \mathcal{S}) &= \sum_{j=1}^L \sum_{k=1}^K \alpha_k l_j (w_k + \rho) C_{i,k}[j] + \sum_{j=2}^{L+1} \beta_j \sum_{m=1}^{j-1} l_m P_C^E[m] \\
&+ \sum_{j=2}^{L+1} \beta_j \sum_{k=1}^K \sum_{m=1}^{j-1} \varepsilon l_m \tilde{P}_{i,k}^E[m] - q \left(\sum_{k=1}^K \sum_{j=1}^L l_j \varepsilon \left(\phi \tilde{P}_{i,k}^E[j] + \tilde{P}_{i,k}^N[j] \right) + \sum_{j=1}^L l_j \left(\phi P_C^E[j] + P_C^N[j] \right) \right) \\
&- \sum_{j=1}^L \psi_j \left(\sum_{k=1}^K l_j \tilde{P}_{i,k}[j] \right) - \sum_{j=1}^L \eta_{i,j} \left(\sum_{k=1}^K s_{i,k}[j] \right) - \sum_{j=1}^L \mu_j \left(\sum_{k=1}^K \varepsilon l_j \tilde{P}_{i,k}^N[j] + l_j P_C^N[j] \right) \\
&- \sum_{j=1}^L l_j \nu_j (P_C^E[j] + P_C^N[j]) - \sum_{j=1}^L \gamma_j \left(\sum_{k=1}^K \sum_{m=1}^j \varepsilon l_m \tilde{P}_{i,k}^E[m] + \sum_{m=1}^j l_m P_C^E[m] \right). \tag{21}
\end{aligned}$$

Let $\tilde{P}_{i,k}^{E*}[j]$, $\tilde{P}_{i,k}^{N*}[j]$, $P_C^{E*}[j]$, $P_C^{N*}[j]$, and $s_{i,k}^*[j]$ denote the solution of subproblem (20) for event j . Using standard optimization techniques and the KKT conditions, the power allocation for signal transmission for user k on subcarrier i for event j is given by

$$\begin{aligned}
\tilde{P}_{i,k}^{E*}[j] &= s_{i,k}[j] P_{i,k}^{E*}[j] = s_{i,k}[j] \left[\frac{W(\alpha_k + \rho)}{\ln(2) \left(\sum_{e=j}^L \gamma_e \varepsilon - \sum_{e=j}^L \beta_{e+1} \varepsilon + q \phi \varepsilon + \psi_j \right) - \frac{1}{\Gamma_{i,k}[j]} } \right]^+ \text{ and} \\
\tilde{P}_{i,k}^{N*}[j] &= s_{i,k}[j] P_{i,k}^{N*}[j] = s_{i,k}[j] \left[\frac{W(\alpha_k + \rho)}{\ln(2) (q \varepsilon + \mu_j \varepsilon + \psi_j) - \frac{1}{\Gamma_{i,k}[j]} - \tilde{P}_{i,k}^{E*}[j]} \right]^+, \tag{22}
\end{aligned}$$

for $\phi < 1$. The power allocation solution in (22) can be interpreted as a *multi-level* water-filling scheme as the water levels of different users can be different. Interestingly, the value of $\tilde{P}_{i,k}^{N*}[j]$ depends on $\tilde{P}_{i,k}^{E*}[j]$. As can be seen in (22), $\tilde{P}_{i,k}^{E*}[j]$ decreases the water-level for calculation of the value of $\tilde{P}_{i,k}^{N*}[j]$. In other words, $\tilde{P}_{i,k}^{E*}[j]$ reduces the amount of energy drawn from the non-renewable source for maximization of energy efficiency. Besides, it can be observed from (22) that the BS does not always consume all available renewable energy in each epoch for maximization of the weighted energy efficiency and the value of q determines at what point the water-level is clipped. On the other hand, in order to obtain the subcarrier allocation, we take the derivative of the subproblem w.r.t. $s_{i,k}[j]$, which yields $\frac{\partial \mathcal{L}_i(\dots)}{\partial s_{i,k}^*[j]} = Q_{i,k}[j] - \eta_{i,j}$, where $Q_{i,k}[j] \geq 0$ is the marginal benefit [36] for allocating subcarrier i to user k for event j and is given by $Q_{i,k}[j] =$

$$W(\alpha_k + \rho) \left(\log_2 \left(1 + \Gamma_{i,k}[j] (P_{i,k}^{E*}[j] + P_{i,k}^{N*}[j]) \right) - \frac{\Gamma_{i,k}[j] (P_{i,k}^{E*}[j] + P_{i,k}^{N*}[j])}{\ln(2) (1 + \Gamma_{i,k}[j] (P_{i,k}^{E*}[j] + P_{i,k}^{N*}[j]))} \right). \tag{23}$$

Thus, the subcarrier selection on subcarrier i in event j is given by

$$s_{i,k}^*[j] = \begin{cases} 1 & \text{if } k = \arg \max_c Q_{i,c}[j] \\ 0 & \text{otherwise} \end{cases}. \tag{24}$$

It can be observed from (23) that only the user who can provide the largest marginal benefit on subcarrier i in epoch j is selected by the resource allocator, for transmission on that subcarrier. This is because the channel gains of different users are generally different due to uncorrelated fading across different users. We note that a larger marginal benefit is not necessarily equivalent to a larger system throughput since the marginal benefit includes a notion of fairness.

After solving the n_F subproblems with identical structure, we calculate the amount of power used for signal processing in each of the two energy sources. We substitute $P_C^N[j] = P_C - P_C^E[j]$ into (20) which yields the following KKT condition for $P_C^{E*}[j]$:

$$\frac{\partial \mathcal{L}_i(\dots)}{\partial P_C^{E*}[j]} = -l_j \sum_{e=j}^L \gamma_e + l_j \sum_{e=j}^L \beta_{e+1} - ql_j \phi + ql_j + \mu l_j \begin{cases} \geq 0, & P_C^{E*}[j] \geq 0 \\ < 0, & \text{otherwise} \end{cases}. \quad (25)$$

It can be observed from (25) that the Lagrangian function $\mathcal{L}_i(\dots)$ is an affine function in $P_C^{E*}[j]$. In other words, the value of $P_C^{E*}[j]$ must be one of the two vertexes of a feasible solution set created by the associated constraints. As a result, the powers used for signal processing drawn from the energy harvester and the non-renewable source are given by

$$P_C^{E*}[j] = \left[\frac{\sum_{a=1}^j E_{in}[a] - \sum_{i=1}^{n_F} \sum_{k=1}^K \sum_{a=1}^j l_a \varepsilon \tilde{P}_{i,k}^{E*}[a] - \sum_{m=1}^{j-1} P_C^E[m] l_m}{l_j} \right]_{0}^{P_C} \text{ and} \quad (26)$$

$$P_C^{N*}[j] = P_C - P_C^{E*}[j], \quad (27)$$

respectively. The numerator of variable $P_C^{E*}[j]$ in (26) represents the residual energy level in the battery, i.e., the vertexes (feasible set) created by the associated constraints on $P_C^{E*}[j]$. Equations (26) and (27) indicate that if the amount of energy in the energy harvester is not sufficient to fully supply the required energy P_C , i.e., $P_C^{E*}[j] < P_C$, then the BS will also draw energy from the non-renewable energy source such that $P_C^{E*}[j] + P_C^{N*}[j] = P_C$.

G. Solution of the Master Dual Problem

For solving the master minimization problem in (19), i.e., to find γ , β , ρ , μ , and ψ for given \mathcal{P} and \mathcal{S} , the gradient method can be used since the dual function is differentiable. The gradient update

equations are given by:

$$\gamma_j(\varsigma + 1) = \left[\gamma_j(\varsigma) - \xi_1(\varsigma) \times \left(\sum_{m=1}^j E_{in}[m] - \sum_{m=1}^j P_C^E[m] l_m \sum_{i=1}^{n_F} \sum_{k=1}^K \sum_{m=1}^j l_m \varepsilon \tilde{P}_{i,k}^E[m] \right) \right]^+, \forall j, \quad (28)$$

$$\beta_r(\varsigma + 1) = \left[\beta_r(\varsigma) - \xi_2(\varsigma) \times \left(E_{\max} + \sum_{m=1}^{r-1} P_C^E[m] l_m - \sum_{m=1}^r E_{in}[m] + \sum_{i=1}^{n_F} \sum_{k=1}^K \sum_{m=1}^r \varepsilon l_m \tilde{P}_{i,k}^E[m] \right) \right]^+, \forall r, \quad (29)$$

$$\rho(\varsigma + 1) = \left[\rho(\varsigma) - \xi_3(\varsigma) \times \left(\sum_{j=1}^L \sum_{k=1}^K \sum_{i=1}^{n_F} l_j C_{i,k}[j] - R_{\min} \right) \right]^+, \quad (30)$$

$$\mu_j(\varsigma + 1) = \left[\mu_j(\varsigma) - \xi_4(\varsigma) \times \left(P_N l_j - \sum_{i=1}^{n_F} \sum_{k=1}^K \varepsilon \tilde{P}_{i,k}^N[j] l_j - P_C^N[j] l_j \right) \right]^+, \forall j, \quad (31)$$

$$\psi_j(\varsigma + 1) = \left[\psi_j(\varsigma) - \xi_5(\varsigma) \times \left(P_{\max} l_j - \sum_{i=1}^{n_F} \sum_{k=1}^K \tilde{P}_{i,k}[j] l_j \right) \right]^+, \forall j, \quad (32)$$

where $j \in \{1, \dots, M + N\}$ and $r \in \{2, \dots, M + N\}$. $\varsigma \geq 0$ and $\xi_u(\varsigma)$, $u \in \{1, \dots, 5\}$, are the iteration index and positive step sizes, respectively. The updated Lagrange multipliers in (28)-(32) are used for solving the subproblems in (19) via updating the resource allocation policies. Updating $\eta_{i,j}$ is not necessary as it has the same value for all users and does not affect the subcarrier allocation in (24). On the other hand, since the transformed problem in (17) is jointly concave w.r.t. the optimization variables and satisfies Slater's constraint qualification [35], the duality gap between dual optimal and relaxed primal optimal is zero and it is guaranteed that the iteration between the master problem and the subproblems converges to the solution of (14) in the main loop, if the chosen step sizes satisfy the infinite travel condition [35], [37].

Note that although the proposed asymptotically (i.e., for a sufficiently large number of subcarriers) optimal offline algorithm requires non-causal knowledge of the channel gains and energy arrivals which may not be available in practice, the performance of the asymptotically optimal offline algorithm serves as an upper bound for any online scheme. Besides, the structure of the asymptotically optimal offline algorithm sheds some light on the design of online algorithms. In the next section, we will address the causality issue by studying two online resource allocation algorithms which utilize causal energy arrival and channel gain information only.

IV. ONLINE RESOURCE ALLOCATION AND SCHEDULING DESIGN

In this section, we study the optimal and a suboptimal online resource allocation algorithms requiring only causal information of energy arrivals and channel states.

A. Optimal Online Solution

In practice, the instantaneous CSI of the users is available at the BS, and can be obtained via feedback and exploiting channel reciprocity in frequency division duplex (FDD) systems and time division duplex (TDD) systems, respectively. Besides, the current energy arrival information for each *energy event* is available after the energy has been harvested. On the contrary, the future CSI and future energy arrival information are not available when the BS computes the resource allocation policy. Therefore, we adopt a statistical approach in the following problem formulation. The optimal online resource allocation policy $\{\mathcal{P}, \mathcal{S}\}$ can be obtained by maximizing the *expected weighted energy efficiency*:

$$\begin{aligned}
& \max_{\mathcal{P}, \mathcal{S}} \mathcal{E}_{\mathbf{F}, \mathbf{E}} \left\{ U_{eff}(\mathcal{P}, \mathcal{S}) \right\} \\
\text{s.t.} \quad & \text{C3, C4, C6, C7, C8, C9} \\
\text{C1: } & \mathcal{E}_{\mathbf{F}, \mathbf{E}} \left\{ \sum_{i=1}^{n_F} \sum_{k=1}^K \int_0^{t_b^E - \delta} \varepsilon_{s_{i,k}}(u) P_{i,k}^E(u) du + \int_0^{t_b^E - \delta} P_C^E(u) du \right\} \leq \sum_{j=0}^{b-1} E_j, \forall b \in \{1, 2, \dots\}, \\
\text{C2: } & \mathcal{E}_{\mathbf{F}, \mathbf{E}} \left\{ \sum_{j=0}^{d(t)} E_j - \sum_{i=1}^{n_F} \sum_{k=1}^K \int_0^t \varepsilon_{s_{i,k}}(u) P_{i,k}^E(u) du - \int_0^t P_C^E(u) du \right\} \leq E_{\max}, 0 \leq t \leq T, \\
\text{C5: } & \mathcal{E}_{\mathbf{F}, \mathbf{E}} \left\{ \sum_{k=1}^K \sum_{i=1}^{n_F} C_{i,k} \right\} \geq R_{\min}, \tag{33}
\end{aligned}$$

where vectors \mathbf{E} and \mathbf{F} in (33) contain the random energy arrivals and channel gains, respectively. Note that although constraints C3, C4, and C6–C9 are the same as in the case of offline algorithm design in (11), the problem formulation here is different from (11). First, C5 specifies now the minimum required *average* data rate of the system. Besides, constraints C1 and C2 are imposed to constrain the *average* energy usage of the system, instead of the instantaneous energy consumption.

For solving (33), we first define $\{\bar{\mathcal{P}}, \bar{\mathcal{S}}\}$ as a feasible resource allocation policy which satisfies constraints C1–C9 in (33). Also, we denote the amount of energy available in the battery at time t by $e(t)$. Then, we apply Theorem 1 to transform the objective function from fractional form into subtractive form. The resulting objective function can be written as

$$\begin{aligned}
J(\bar{\mathcal{P}}, \bar{\mathcal{S}}, t, e(t)) = & \mathcal{E}_{\mathbf{F}, \mathbf{E}} \left\{ \sum_{k=1}^K \alpha_k \sum_{i=1}^{n_F} W \int_t^T s_{i,k}(\tau) C_{i,k}(\tau) d\tau - q \left[\int_t^T (\phi P_C^E(\tau) + P_C^N(\tau)) d\tau \right. \right. \\
& \left. \left. + \sum_{k=1}^K \sum_{i=1}^{n_F} \int_t^T s_{i,k}(\tau) \varepsilon \left(P_{i,k}^E(\tau) \phi + P_{i,k}^N(\tau) \right) d\tau \right] \right\}, \tag{34}
\end{aligned}$$

where $t = 0$, $C_{i,k}(\tau) = \log_2 \left(1 + P_{i,k}(\tau) \Gamma_{i,k}(\tau) \right)$, and q can be found via a similar approach as described in Table I. After that, we can approximate the integrals in (33) as Riemann sums of Ξ

equally spaced intervals with an interval width of $\epsilon = \frac{T}{\Xi}$. Thus, for a sufficiently small value of ϵ , we can discretize the integrals and the objective function in (33) can be parameterized by t [38]:

$$J(\bar{\mathcal{P}}, \bar{\mathcal{S}}, m\epsilon, e(m\epsilon)) = \mathcal{E}_{\mathbf{F}, \mathbf{E}} \left\{ \sum_{k=1}^K \alpha_k \sum_{i=1}^{n_F} W \sum_{v=m}^{\Xi-1} \epsilon s_{i,k}(v\epsilon) C_{i,k}(v\epsilon) - q\epsilon \left[\sum_{v=m}^{\Xi-1} \left(\phi P_C^E(v\epsilon) + P_C^N(v\epsilon) \right) + \sum_{k=1}^K \sum_{i=1}^{n_F} \sum_{v=m}^{\Xi-1} \epsilon s_{i,k}(v\epsilon) \varepsilon \left(P_{i,k}^E(v\epsilon) \phi + P_{i,k}^N(v\epsilon) \right) \right] \right\}, \quad (35)$$

where $t = m\epsilon$ for $m = \{0, 1, 2, \dots, \Xi - 1\}$. Then, the optimal *cost-to-go* function [39], [40] at time t is given by

$$J^*(m\epsilon, e(m\epsilon)) = \max_{\bar{\mathcal{P}}, \bar{\mathcal{S}}} J(\bar{\mathcal{P}}, \bar{\mathcal{S}}, m\epsilon, e(m\epsilon)). \quad (36)$$

By applying Bellmans equations and backward induction [39], [40], it can be shown that the optimal resource allocation policy $\{\bar{\mathcal{P}}^*, \bar{\mathcal{S}}^*\}$ for solving (33) must satisfy the following dynamic programming (DP) equation:

$$J^*(m\epsilon, e(m\epsilon)) = \max_{\bar{\mathcal{P}}, \bar{\mathcal{S}}} \left\{ \epsilon \sum_{k=1}^K \alpha_k \sum_{i=1}^{n_F} W s_{i,k}(m\epsilon) C_{i,k}(m\epsilon) - q\epsilon \left[\left(\phi P_C^E(m\epsilon) + P_C^N(m\epsilon) \right) \right] - q\epsilon \left[\sum_{k=1}^K \sum_{i=1}^{n_F} s_{i,k}(m\epsilon) \varepsilon \left(P_{i,k}^E(m\epsilon) \phi + P_{i,k}^N(m\epsilon) \right) \right] + J^*((m+1)\epsilon, e((m+1)\epsilon)) \right\}, \quad \forall m. \quad (37)$$

In other words, the optimal online resource allocation policy in (33) can be obtained by solving (37) via standard DP [39], [40]. To summarize the implementation of the optimal online resource allocation algorithm, at time $t = 0$, the BS computes the resource allocation policy via standard DP. Note that the policy is a function of CSI $H_{i,k}(t)$ and the energy level $e(t)$ in the battery. For time $t > 0$, the BS updates $H_{i,k}(t)$ and $e(t)$ and performs resource allocation based on $\{\bar{\mathcal{P}}^*, \bar{\mathcal{S}}^*\}$ at each discretized time interval $t = m\epsilon$ for each value of m .

B. Suboptimal Online Solution

In the last section, we introduced the optimal online resource allocation policy which can be obtained via DP. Yet, it is well known that DP suffers from the “*curse of dimensionality*”. Specifically, the search space for the optimal solution increases exponentially w.r.t. the number of users and subcarriers. Hence, in practice, DP is not applicable for the considered system due to the huge computational complexity and memory requirement. In the following, we propose a suboptimal online resource allocation algorithm which is inspired by the asymptotically optimal offline resource allocation derived in Section III-C. In particular, the proposed suboptimal resource allocation algorithm is *event-driven*

and each computation is triggered by a change in fading level or an energy arrival. In other words, the proposed suboptimal online algorithm requires only causal system information and the statistics of the involved events which leads to a lower complexity compared to the optimal online solution. Note that in order to emphasize the similarity between the offline algorithm and the proposed suboptimal online algorithm, with a slight abuse of notation, we use a similar notation for both algorithms.

Suboptimal Algorithm: The structure of the offline resource allocation algorithm in Section III depends on the length of each epoch. However, this knowledge is unavailable at the BS due to causality constraints. As a compromise solution, we focus on the statistical average of the length of each event. We define the average length of each epoch as $\overline{L_E}$ and there are $Z = \lfloor \frac{T}{\overline{L_E}} + 1 \rfloor$ events in T seconds on average. In practice, the value of $\overline{L_E}$ can be estimated by long term channel and energy arrival measurements. Besides, to simplify the resource allocation algorithm, we assume that the resource allocation policy is constant in each epoch which was shown to be optimal for the case of offline algorithm design. As a result, we can directly formulate the resource allocation design problem by using a discrete representation. Without loss of generality, we focus on the resource allocation algorithm design for epoch j . Then, the *weighted average system throughput* and the *total weighted energy consumption* in epoch j are given by

$$U(\mathcal{P}_j, \mathcal{S}_j) = \sum_{k=1}^K \alpha_k \sum_{i=1}^{n_F} \overline{L_E} C_{i,k}[j] \text{ and}$$

$$U_{TP}(\mathcal{P}_j, \mathcal{S}_j) = \overline{L_E} \left(\phi P_C^E[j] + P_C^N[j] \right) + \sum_{k=1}^K \sum_{i=1}^{n_F} \overline{L_E} \varepsilon \left(\tilde{P}_{i,k}^E[j] \phi + \tilde{P}_{i,k}^N[j] \right), \quad (38)$$

respectively. The resource allocation policy, $\mathcal{P}_j = \{\tilde{P}_{i,k}^E[j], \tilde{P}_{i,k}^N[j], P_C^E[j], P_C^N[j]\}$, $\mathcal{S}_j = \{s_{i,k}[j]\}$, which maximizes the weighted energy efficiency in epoch j can be obtained by solving

$$\begin{aligned} & \max_{\mathcal{P}_j, \mathcal{S}_j} \frac{U(\mathcal{P}_j, \mathcal{S}_j)}{U_{TP}(\mathcal{P}_j, \mathcal{S}_j)} \quad (39) \\ \text{s.t.} \quad & \text{C1: } \sum_{i=1}^{n_F} \sum_{k=1}^K \overline{L_E} \varepsilon \tilde{P}_{i,k}^E[j] + \overline{L_E} P_C^E[j] \leq E[j], \\ & \text{C3: } \sum_{i=1}^{n_F} \sum_{k=1}^K \overline{L_E} \varepsilon \tilde{P}_{i,k}^N[j] + \overline{L_E} P_C^N[j] \leq P_N \overline{L_E}, \quad \text{C4: } \overline{L_E} P_C^E[j] + \overline{L_E} P_C^N[j] = \overline{L_E} P_C, \\ & \text{C5: } \sum_{k=1}^K \sum_{i=1}^{n_F} \sum_{j=1}^L \overline{L_E} C_{i,k}[j] \geq \frac{R_{\min}}{Z}, \quad \text{C6: } \sum_{i=1}^{n_F} \sum_{k=1}^K \overline{L_E} \tilde{P}_{i,k}[j] \leq \overline{L_E} P_{\max}, \\ & \text{C7: } 0 \leq s_{i,k}[j] \leq 1, \forall i, k, \quad \text{C8: } \sum_{k=1}^K s_{i,k}[j] \leq 1, \forall i, \quad \text{C9: } P_{i,k}^N[j], P_{i,k}^E[j], P_C^N[j], P_C^E[j] \geq 0, \forall i, k, \end{aligned}$$

where $E[j]$ is the amount of energy available in the battery in epoch j . It captures the joint effect of channel fluctuations, energy arrivals, and resource allocation in the previous epochs on the energy availability in epoch j . This information is available at the BS by monitoring the amount of energy consumed and harvested in the past epochs. Note that the battery overflow constraint C2 is not imposed in the suboptimal online problem formulation (39) for solution tractability. In practice, the amount of energy exceeding the battery storage will be discharged and not stored. The performance loss caused by the above problem formulation compared to the optimal one will be investigated in the simulation section.

To solve the optimization problem in (39), we can use Theorem 1 (objective function transformation) and Algorithm 1 (iterative algorithm) which were introduced in Section III-D. In particular, in each iteration of the main loop, cf. Table I, we solve the following optimization problem for a given parameter q :

$$\begin{aligned} \max_{\mathcal{P}_j, \mathcal{S}_j} \quad & U(\mathcal{P}_j, \mathcal{S}_j) - qU_{TP}(\mathcal{P}_j, \mathcal{S}_j) \\ \text{s.t.} \quad & \text{C1, C3–C9.} \end{aligned} \quad (40)$$

The above optimization problem can be proved to be jointly concave w.r.t. the optimization variables by using a similar approach as in the Appendix. Similar to the offline resource allocation problem, we solve (40) by dual decomposition. The Lagrangian of (40) is given by

$$\begin{aligned} \mathcal{L}(\gamma, \psi, \rho, \boldsymbol{\eta}, \mu, \nu, \mathcal{P}_j, \mathcal{S}_j) = & \sum_{k=1}^K \alpha_k \sum_{i=1}^{n_F} \overline{L}_E(w_k + \rho) C_{i,k}[j] - \rho \frac{R_{\min}}{Z} - q \overline{L}_E \left((\phi P_C^E[j] + P_C^N[j]) \right. \\ & + \left. \sum_{k=1}^K \sum_{i=1}^{n_F} \varepsilon \left(\tilde{P}_{i,k}^E[j] \phi + \tilde{P}_{i,k}^N[j] \right) \right) - \gamma \left(\sum_{i=1}^{n_F} \sum_{k=1}^K \overline{L}_E \varepsilon \tilde{P}_{i,k}^E[j] + \overline{L}_E P_C^E[j] - E[j] \right) \\ & - \mu \overline{L}_E \left(\sum_{i=1}^{n_F} \sum_{k=1}^K \varepsilon \tilde{P}_{i,k}^N[j] + P_C^N[j] - P_N \right) - \nu \overline{L}_E \left(P_C^E[j] + P_C^N[j] - P_C \right) \\ & - \psi \overline{L}_E \left(\sum_{i=1}^{n_F} \sum_{k=1}^K \tilde{P}_{i,k}[j] - P_{\max} \right) - \sum_{i=1}^{n_F} \eta_i \left(\sum_{k=1}^K s_{i,k}[j] - 1 \right), \end{aligned} \quad (41)$$

where γ , μ , ν , ρ , and ψ are the scalar Lagrange multipliers associated with constraints C1 and C3–C6 in (39), respectively. $\boldsymbol{\eta}$ is the Lagrange multiplier vector for subcarrier usage constraint C8 and has elements $\eta_i, i \in \{1, \dots, n_F\}$. Thus, the dual problem is given by

$$\min_{\gamma, \psi, \rho, \boldsymbol{\eta}, \mu \geq 0} \max_{\mathcal{P}_j, \mathcal{S}_j} \mathcal{L}(\gamma, \psi, \rho, \boldsymbol{\eta}, \mu, \nu, \mathcal{P}_j, \mathcal{S}_j). \quad (42)$$

Dual Decomposition and Solution of Optimization Problem: By using dual decomposition and following a similar approach as in (19)-(27), the resource allocation policy can be obtained via an iterative approach. For a given set of Lagrange multipliers $\{\gamma, \psi, \rho, \eta, \mu\}$, the power allocation $\mathcal{P}_j^* = \{\tilde{P}_{i,k}^{E*}[j], \tilde{P}_{i,k}^{N*}[j], P_C^{E*}[j], P_C^{N*}[j]\}$ and the subcarrier allocation $\mathcal{S}_j^* = \{s_{i,k}^*[j]\}$ for dual problem (42) for the signals from the BS to user k in subcarrier i in epoch j are given by

$$\tilde{P}_{i,k}^{E*}[j] = s_{i,k}[j]P_{i,k}^{E*}[j] = s_{i,k}[j] \left[\frac{W(\alpha_k + \rho)}{(\ln(2)(q\phi\varepsilon + \psi + \gamma))} - \frac{1}{\Gamma_{i,k}[j]} \right]^+ \quad (43)$$

$$\tilde{P}_{i,k}^{N*}[j] = s_{i,k}[j]P_{i,k}^{N*}[j] = s_{i,k}[j] \left[\frac{W(\alpha_k + \rho)}{(\ln(2)(q\varepsilon + \mu\varepsilon + \psi))} - \frac{1}{\Gamma_{i,k}[j]} - \tilde{P}_{i,k}^{E*}[j] \right]^+, \quad (44)$$

$$s_{i,k}^*[j] = \begin{cases} 1 & \text{if } k = \arg \max_c Q_{i,c}[j] \\ 0 & \text{otherwise} \end{cases}, \quad (45)$$

$$P_C^{E*}[j] = \left[\frac{E[j] - \overline{L_E} \tilde{P}_{i,k}^{E*}[j]}{\overline{L_E}} \right]^{P_C}, \text{ and } P_C^{N*}[j] = P_C - P_C^{E*}[j], \quad (46)$$

where $\phi < 1$ and $Q_{i,k}[j]$ is defined in (23). It can be observed that the proposed suboptimal online solution (43)–(46) shares some common properties with the asymptotically optimal offline solution in (22)–(27). In particular, the BS will prefer to first consume energy from the energy harvester for $\phi < 1$. If the energy provided by the energy harvester is not sufficient for achieving the maximum weighted energy efficiency of the system, the BS will start to consume energy from the non-renewable energy source. However, here, the value of q in (43) and (44) is calculated w.r.t. the average epoch length $\overline{L_E}$. On the contrary, the value of q in (17) captures the effects of all channel gains and energy arrivals in the time horizon of T seconds.

We can update the set of Lagrange multipliers $\{\gamma, \psi, \rho, \mu\}$ for a given $\mathcal{P}_j, \mathcal{S}_j$ by using the gradient method, since the dual function is differentiable. The gradient update equations are given by:

$$\gamma(\varsigma + 1) = \left[\gamma(\varsigma) - \xi_1(\varsigma) \times \left(E[j] - \sum_{i=1}^{n_F} \sum_{k=1}^K \overline{L_E} \tilde{P}_{i,k}^{E*}[j] - \overline{L_E} P_C^{E*}[j] \right) \right]^+, \quad (47)$$

$$\mu(\varsigma + 1) = \left[\mu(\varsigma) - \xi_2(\varsigma) \times \left(\overline{L_E} P_N - \sum_{i=1}^{n_F} \sum_{k=1}^K \overline{L_E} \tilde{P}_{i,k}^{N*}[j] - \overline{L_E} P_C^{N*}[j] \right) \right]^+, \quad (48)$$

$$\rho(\varsigma + 1) = \left[\rho(\varsigma) - \xi_3(\varsigma) \times \left(\sum_{k=1}^K \sum_{i=1}^{n_F} \sum_{j=1}^L \overline{L_E} C_{i,k}[j] - \frac{R_{\min}}{Z} \right) \right]^+, \quad (49)$$

$$\psi(\varsigma + 1) = \left[\psi(\varsigma) - \xi_4(\varsigma) \times \left(\overline{L_E} P_{\max} - \left(\sum_{i=1}^{n_F} \sum_{k=1}^K \overline{L_E} \tilde{P}_{i,k}^{E*}[j] \right) \right) \right]^+. \quad (50)$$

Similar to the case of offline algorithm design, updating η is not necessary since it will not affect the subcarrier allocation in (45). A summary of the overall algorithm is given in Table I. In each iteration of the main loop, we solve (40) in line 7 of Algorithm 1 for a given parameter q via dual decomposition, cf. (43)-(50). Then, we update parameter q and use it for solving (40) in the next iteration. This procedure is repeated until the proposed algorithm converges.

We now analyze the complexity of the proposed suboptimal online algorithm. The proposed iterative algorithm requires the execution of two nested loops in each event. The complexity of the outer loop, i.e., Algorithm 1, can be proved to be linear in n_F [41]. On the other hand, the inner loop optimization problem in (40) is jointly concave w.r.t. the optimization variables. As a result, the solution for the problem formulation in (42) can be obtained with a complexity quadratically in each epoch for the worst case, i.e., the complexity is $\mathcal{O}(n_F \times K^2)$ where K^2 is due to the worst case complexity in calculating (45). As a result, the complexity of the proposed algorithm for an average of Z events in T seconds is $\mathcal{O}(n_F \times K^2 \times Z)$.

V. RESULTS AND DISCUSSIONS

In this section, we evaluate the system performance for the proposed resource allocation and scheduling algorithms using simulations. A micro-cell system with radius 500 m is considered. The number of subcarriers is $n_F = 128$ with carrier center frequency 2.5 GHz, system bandwidth $\mathcal{B} = 5$ MHz, and $\alpha_k = 1, \forall k$. Each subcarrier has a bandwidth of 39 kHz and the noise variance is $\sigma_z^2 = -128$ dBm. The 3GPP urban path loss model is used [42] with a reference distance of $d_0 = 35$ m. The K desired users are uniformly distributed between the reference distance and the cell boundary. The small scale fading coefficients of the BS-to-user links are generated as independent and identically distributed (i.i.d.) Rayleigh random variables. The multipath channel characteristic of each user is assumed to follow the power delay profile according of the LTE extended pedestrian A channel model [43]. The static circuit power consumption is set to $P_C = 40$ dBm [44]. Unless specified otherwise, the minimum data rate requirement of the system is $R_{\min} = 5$ Mbits/s. We assume a transmission duration of $T = 10$ seconds. The maximum transmit power allowance P_{\max} will be specified in each case study. The energy harvester has a maximum energy storage of $E_{\max} = 500$ J and an initial energy $E_0 = 0$ J in the battery¹¹. The amount of energy that can be harvested by the energy harvester in each energy epoch is assumed to be a fixed amount of 5 J. Then, the energy harvesting rate of the system is $5\lambda_E$ Joule/s. The value of ϕ is set to $\phi = 0.01$ to account for the preference for harvested

¹¹The values of the battery capacity and energy arrival (/harvesting) rates used in the paper are for illustration purpose. In practice, the choice of battery capacity should scale with the energy arrival (/harvesting) rates and the cell size.

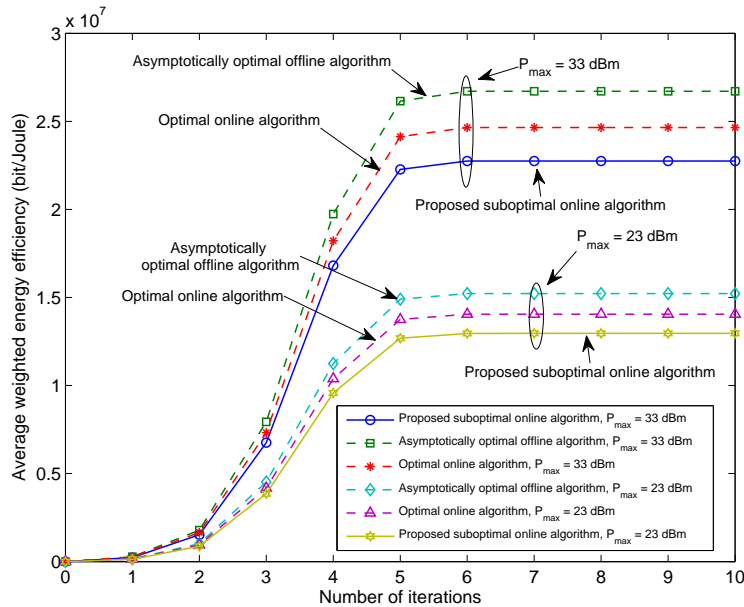


Fig. 3. Average weighted energy efficiency (bit-per-Joule) versus number of iterations with different maximum transmit power allowances, P_{\max} , for $K = 5$ users, a maximum power supplied by the non-renewable source $P_N = 50$ dBm, and an energy harvesting rate of 20 Joule/s.

energy. The conference time for the multipath fading coefficients of each fading block is 200 ms. We set $\epsilon = 0.01$ for calculating the *optimal online resource allocation policy* via DP. Furthermore, we assume a power efficiency of 35% in the PA, i.e., $\epsilon = \frac{1}{0.35} = 2.8571$. The average weighted system energy efficiency is obtained by counting the number of weighted bits which are successfully decoded by the receiver over the total energy consumption averaged over the small scale fading. Note that if the resource allocator is unable to guarantee the minimum data rate R_{\min} in T , we set the weighted energy efficiency and the average system capacity for these channel realizations to zero to account for the corresponding failure. Besides, unless further specified, in the following results, the “number of iterations” refers to the number of iterations of Algorithm 1 in Table I.

A. Convergence of Proposed Iterative Algorithm

Figure 3 illustrates the evolution of the proposed suboptimal online iterative algorithm for different maximum transmit power allowances, P_{\max} , $K = 5$ users, and an energy harvesting rate of 20 Joule/s. The results in Figure 3 were averaged over 10^5 independent adaptation processes where each adaptation process involves a different realization of the path loss and the small scale fading. It can be observed that on average, in each case, the suboptimal iterative algorithm converges to above 83% and 90% of the weighted energy efficiency of the asymptotically *optimal offline* and *optimal online* algorithms within 5 iterations, respectively. On the other hand, the inner loop for solving (39) converges within 5 iterations in each event. In other words, on average the overall algorithm requires in total around $5 \times 5 \times Z$ iterations (inner loops and outer loops in T seconds) to converge where Z is the average

number of events during T seconds.

In the following case studies, we set the number of iterations in the proposed suboptimal algorithm to 5.

B. Energy Efficiency and Average Capacity versus Energy Harvesting Rates

Figure 4 illustrates the average weighted energy efficiency versus the energy harvesting rate, for different maximum transmit power allowances, P_{\max} , and $K = 5$ users. It can be observed that the average weighted energy efficiency of the proposed suboptimal algorithm increases rapidly for increasing energy harvesting rate. This is because more energy is available at the energy harvester as the energy harvesting rate increases. As a result, the resource allocator reduces its reliance on the energy supplied by the non-renewable energy source by exploiting a larger amount of energy from the energy harvester. For comparison, Figure 4 also contains results for both the *optimal online* algorithm and the asymptotically *optimal offline* algorithm which serve as performance benchmarks. It can be observed that the proposed suboptimal algorithm has a performance close to that of the benchmark algorithms in all considered scenarios. In particular, the performance of the proposed suboptimal algorithm approaches the benchmark schemes in both the low and the high energy harvesting rate regimes. This is because in the low energy harvesting rate regime, the energy supplied by the energy harvester is very limited. Thus, the BS has to rely mainly on the non-renewable source for maintaining normal operation and the influence of the energy harvester on system performance becomes insignificant. In the other extreme, the high energy harvesting rate converts the energy harvester into a continuous energy source. As a result, knowledge about the future energy arrivals in the asymptotically optimal offline algorithm becomes less valuable for resource allocation purpose, since there is always sufficient harvested energy for system operation in each epoch.

Figure 5 depicts the average weighted energy efficiency (bit-per-Joule) versus energy harvesting rate for the proposed suboptimal algorithm for different values of maximum non-renewable energy supply P_N and maximum transmit power allowances P_{\max} . Figure 5 provides useful insight for system design as far as the choice of the maximum output power for the non-renewable energy supply is concerned. It can be observed that for all considered scenarios, a higher value of P_N achieves a better average weighted energy efficiency. This is because a larger value of P_N allows a higher flexibility in resource allocation since the non-renewable energy can be used as a supplement for the harvested energy whenever there is insufficient energy in the battery. However, there is a diminishing return in performance as P_N increases in the high energy harvesting rate regime. This is due to the fact that for a large value of energy harvesting rate, the BS is able to consume a large amount of energy from the

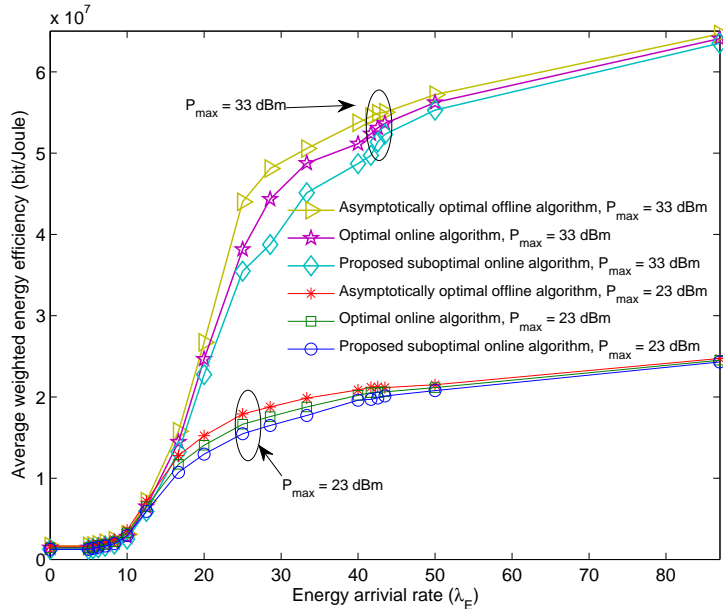


Fig. 4. Average weighted energy efficiency (bit-per-Joule) versus energy harvesting rate (Joule-per-second) for the proposed suboptimal algorithm and the benchmark schemes for different values of maximum transmit power allowance, P_{\max} . The maximum power supplied by the non-renewable source is set to $P_N = 50$ dBm.

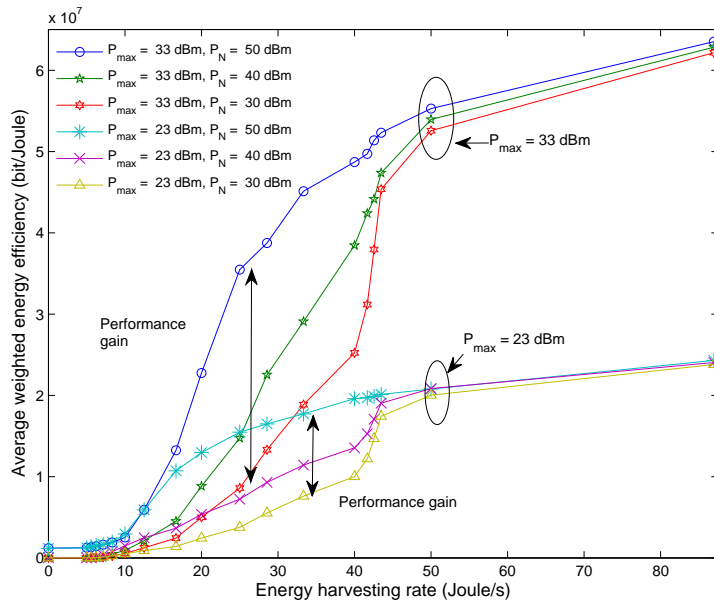


Fig. 5. Average weighted energy efficiency (bit-per-Joule) versus energy harvesting rate (Joule-per-second) for the proposed suboptimal algorithm for different values for maximum non-renewable energy supply, P_N , and maximum transmit power allowance, P_{\max} . The double sided arrows represent the performance gains due to larger values of P_N .

energy harvester which reduces the dependence on the non-renewable energy source. As a result, a small output power of the non-renewable energy supply is only preferable when the energy harvester is able to harvest a large amount of energy.

Figure 6 shows the average system capacity versus energy harvesting rate for $K = 5$ users and different maximum transmit power allowances P_{\max} . We compare the system performance of the

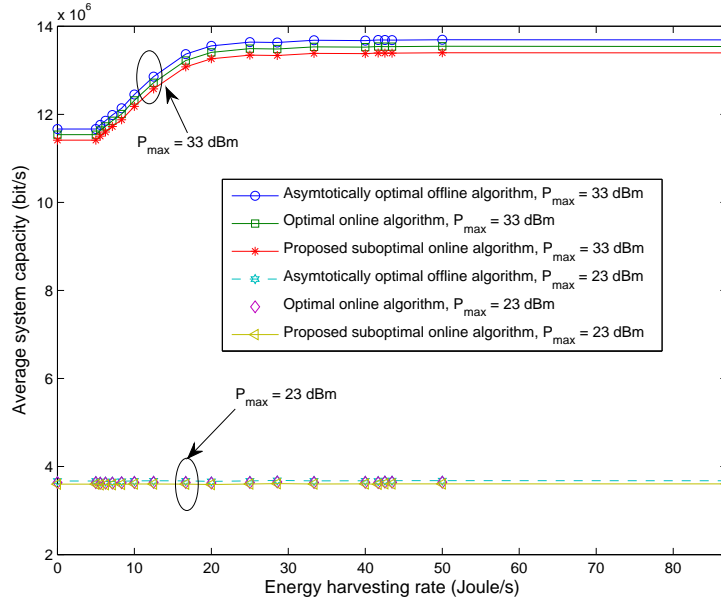


Fig. 6. Average system capacity (bit/s) versus energy harvesting rate (Joule-per-second) for the proposed suboptimal algorithm and the benchmark schemes for different values of maximum transmit power allowance, P_{\max} . The maximum power supplied by the non-renewable source is set to $P_N = 50$ dBm.

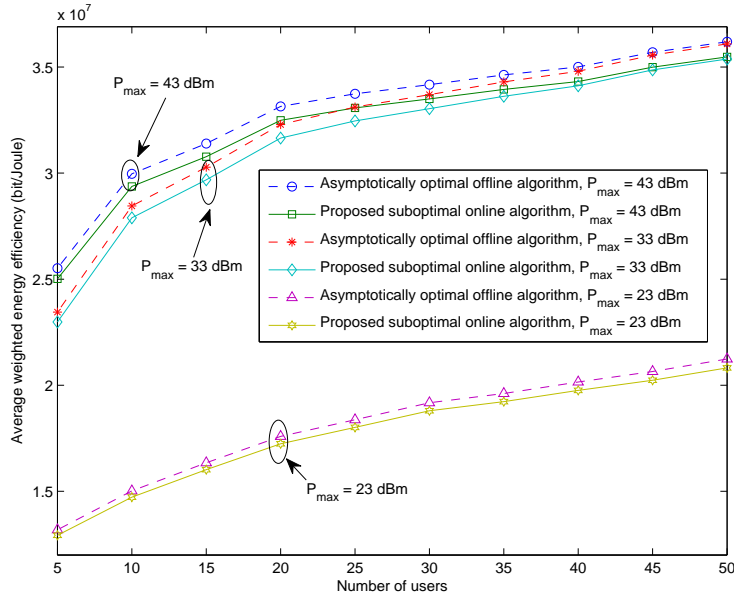


Fig. 7. Average weighted energy efficiency (bit-per-Joule) versus the number of users K for the proposed suboptimal algorithm and the asymptotically optimal offline scheme for different values of maximum transmit power allowance, P_{\max} , and an energy harvesting rate of 20 Joule/s. The maximum power supplied by the non-renewable source is set to $P_N = 50$ dBm.

proposed suboptimal algorithm again with the two aforementioned benchmark schemes. It can be observed that the average system capacity of the proposed suboptimal algorithm approaches a constant in the high energy harvesting rate regime for the case of $P_{\max} = 33$ dBm. This is because the proposed suboptimal algorithm clips the transmit power at the BS in order to maximize the weighted system

energy efficiency. However, when the maximum transmit power allowance is small, i.e., $P_{\max} = 23$ dBm, the system capacity performance gains due to a high energy harvesting rate are quickly saturated for all schemes since the system capacity is always limited by the small amount of radiated power in the RF. On the other hand, we note that, as expected, the benchmark schemes achieve a higher average system capacity than the proposed suboptimal online algorithm, since the proposed suboptimal scheme utilizes only the CSI of the current epoch.

C. Energy Efficiency versus Number of Users

Figure 7 depicts the weighted energy efficiency versus the number of users. Different maximum transmit power allowances P_{\max} at the BS are assumed for an energy harvesting rate of 20 Joule/s. Note that the performance of the optimal online algorithm is not shown here since the computational complexity in solving (37) becomes prohibitive for a large number of users K . It can be observed that in all considered cases, the performances of the proposed suboptimal online algorithm and the asymptotically optimal offline algorithm scale with the number of users with a similar slope. In other words, the proposed suboptimal online algorithm is able to exploit multiuser diversity (MUD) for enhancing the system performance. Indeed, MUD introduces an extra power/energy gain [45, Chapter 6.6] to the system which facilitates further energy savings. On the other hand, there is a diminishing return in the weighted energy efficiency for increasing the maximum transmit power allowance from $P_{\max} = 33$ dBm to $P_{\max} = 43$ dBm, since both schemes are not willing to consume exceedingly large amounts of energy for signal transmission.

VI. CONCLUSIONS

In this paper, we formulated the resource allocation algorithm design for OFDMA systems with hybrid energy harvesting BSs as a non-convex optimization problem, in which the circuit energy consumption, the finite battery storage capacity, and a minimum system data rate requirement were taken into consideration. We first studied the structure of the asymptotically optimal offline resource allocation algorithm by assuming non-causal channel gain and energy arrival knowledge. Then, the derived offline solution served as a building block for the design of a practical close-to-optimal online resource allocation algorithm requiring only causal system knowledge. Simulation results did not only unveil the achievable maximum weighted energy efficiency, but showed also that the proposed suboptimal online algorithm achieves a close-to-optimal performance within a small number of iterations. Interesting topics for future work include studying the effects of imperfect CSI and energy leakage.

APPENDIX-PROOF OF LEMMA 1

The proof of Lemma 1 is divided into two parts. In the first part, we prove the concavity of the optimization problem in (14). Then, in the second part, we prove a necessary condition for the optimal resource allocation policy based on the result in part one.

A. Proof of the Concavity of the Transformed Problem in (14)

We first consider the concavity of the objective function on a per subcarrier basis w.r.t. all optimization variables. For the sake of notational simplicity, we define the receive channel gain-to-noise ratio (CNR) and the channel capacity between the BS and user k on subcarrier i at time instant t as $\Gamma_{i,k}(t) = \frac{|H_{i,k}(t)|^2 g_k(t)}{N_0 W}$ and $C_{i,k}(t) = s_{i,k}(t) W \log_2(1 + \frac{\tilde{P}_{i,k}(t) \Gamma_{i,k}(t)}{s_{i,k}(t)})$, respectively. Let the objective function in (14) on subcarrier i for user k at time instant t be $f_{i,k}(t, \mathcal{P}, \mathcal{S}) = \alpha_k C_{i,k}(t) - q[\varepsilon \phi \tilde{P}_{i,k}^E(t) + \varepsilon \tilde{P}_{i,k}^N(t) + \phi P_C^E(t) + P_C^N(t)]$. Then, we define $\mathbf{H}(f_{i,k}(t, \mathcal{P}, \mathcal{S}))$ and $\varphi_1, \varphi_2, \dots$, and φ_5 as the Hessian matrix of function $f_{i,k}(t, \mathcal{P}, \mathcal{S})$ and the five eigenvalues of $\mathbf{H}(f_{i,k}(t, \mathcal{P}, \mathcal{S}))$, respectively. The Hessian of function $f_{i,k}(t, \mathcal{P}, \mathcal{S})$ and the corresponding eigenvalues are given by

$$\mathbf{H}(f_{i,k}(t, \mathcal{P}, \mathcal{S})) = \begin{bmatrix} \Lambda_{i,k}(t) & \Lambda_{i,k}(t) & \Psi_{i,k}(t) & 0 & 0 \\ \Lambda_{i,k}(t) & \Lambda_{i,k}(t) & \Psi_{i,k}(t) & 0 & 0 \\ \Psi_{i,k}(t) & \Psi_{i,k}(t) & \Upsilon_{i,k}(t) & 0 & 0 \\ 0 & 0 & 0 & 0 & 0 \\ 0 & 0 & 0 & 0 & 0 \end{bmatrix}, \varphi_1 = \varphi_2 = \varphi_3 = \varphi_4 = 0,$$

$$\text{and } \varphi_5 = \frac{-\Gamma_{i,k}^2(t)(W\alpha_k)[(\tilde{P}_{i,k}^E(t) + \tilde{P}_{i,k}^N(t))^2 + 2s_{i,k}^2(t)]/\ln(2)/s_{i,k}(t)}{(s_{i,k}(t) + \Gamma_{i,k}(t)[\tilde{P}_{i,k}^E(t) + \tilde{P}_{i,k}^N(t)])^2} \leq 0, \quad (51)$$

respectively, where $\Lambda_{i,k}(t) = \frac{-\Gamma_{i,k}^2(t)(W\alpha_k)s_{i,k}(t)/\ln(2)}{(s_{i,k}(t) + \Gamma_{i,k}(t)[\tilde{P}_{i,k}^E(t) + \tilde{P}_{i,k}^N(t)])^2}$, $\Psi_{i,k}(t) = \frac{-\Gamma_{i,k}^2(t)(W\alpha_k)s_{i,k}(t)/\ln(2)}{(s_{i,k}(t) + \Gamma_{i,k}(t)[\tilde{P}_{i,k}^E(t) + \tilde{P}_{i,k}^N(t)])^2}$, and $\Upsilon_{i,k}(t) = \frac{-\Gamma_{i,k}^2(t)(W\alpha_k)(\tilde{P}_{i,k}^E(t) + \tilde{P}_{i,k}^N(t))/\ln(2)/s_{i,k}(t)}{(s_{i,k}(t) + \Gamma_{i,k}(t)[\tilde{P}_{i,k}^E(t) + \tilde{P}_{i,k}^N(t)])^2}$. Hence, $\mathbf{H}(f_{i,k}(t, \mathcal{P}, \mathcal{S}))$ is a negative semi-definite matrix since $\varphi_\varrho \leq 0, \varrho = 1, \dots, 5$. Therefore, $f_{i,k}(t, \mathcal{P}, \mathcal{S})$ is jointly concave w.r.t. optimization variables $\tilde{P}_{i,k}^E(t), \tilde{P}_{i,k}^N(t), P_C^E(t), P_C^N(t)$, and $s_{i,k}(t)$ at time instant t . Besides, the integration of $f_{i,k}(t, \mathcal{P}, \mathcal{S})$ over t and the sum of $f_{i,k}(t, \mathcal{P}, \mathcal{S})$ over indices k and i preserve the concavity of the objective function in (14) [35]. On the other hand, constraints C1-C9 in (14) span a convex feasible set, and thus the transformed problem is a concave optimization problem.

B. Optimality of Constant Resource Allocation Policy in each Epoch

Without loss of generality, we consider the time interval $[t_1, t_2)$ of epoch 1 and time instant τ_1 , where $t_1 \leq \tau_1 < t_2$. Suppose an adaptive resource allocation policy is adopted in $t_1 \leq \tau_1 < t_2$ such that two constant resource allocation policies, $\{\mathcal{P}_1, \mathcal{S}_1\}$ and $\{\mathcal{P}_2, \mathcal{S}_2\}$, are applied in $t_1 \leq t < \tau_1$ and $\tau_1 \leq t < t_2$, respectively. We assume that $\{\mathcal{P}_1, \mathcal{S}_1\}$ and $\{\mathcal{P}_2, \mathcal{S}_2\}$ are feasible solutions to (14)

while $\mathcal{P}_1 \neq \mathcal{P}_2$ and $\mathcal{S}_1 \neq \mathcal{S}_2$. Now, we define a third resource allocation policy $\{\mathcal{P}_3, \mathcal{S}_3\}$ such that $\mathcal{P}_3 = \frac{\mathcal{P}_1(\tau_1 - t_1) + \mathcal{P}_2(t_2 - \tau_1)}{t_2 - t_1}$ and $\mathcal{S}_3 = \frac{\mathcal{S}_1(\tau_1 - t_1) + \mathcal{S}_2(t_2 - \tau_1)}{t_2 - t_1}$. Note that arithmetic operations between any two resource allocation policies are defined element-wise. Then, we apply resource allocation policy¹² $\{\mathcal{P}_3, \mathcal{S}_3\}$ to the entire *epoch 1* and integrate $f_{i,k}(t, \mathcal{P}, \mathcal{S})$ over time interval $[t_1, t_2)$ which yields:

$$\begin{aligned}
& \int_{t_1}^{t_2} \sum_{i=1}^{n_F} \sum_{k=1}^K f_{i,k}(t, \mathcal{P}_3, \mathcal{S}_3) dt \\
& \stackrel{(a)}{\geq} \int_{t_1}^{t_2} \left(\frac{\tau_1 - t_1}{t_2 - t_1} \sum_{i=1}^{n_F} \sum_{k=1}^K f_{i,k}(t, \mathcal{P}_1, \mathcal{S}_1) + \frac{t_2 - \tau_1}{t_2 - t_1} \sum_{i=1}^{n_F} \sum_{k=1}^K f_{i,k}(t, \mathcal{P}_2, \mathcal{S}_2) \right) dt \\
& = (\tau_1 - t_1) \sum_{i=1}^{n_F} \sum_{k=1}^K f_{i,k}(t, \mathcal{P}_1, \mathcal{S}_1) + (t_2 - \tau_1) \sum_{i=1}^{n_F} \sum_{k=1}^K f_{i,k}(t, \mathcal{P}_2, \mathcal{S}_2) \\
& = \int_{t_1}^{\tau_1} \sum_{i=1}^{n_F} \sum_{k=1}^K f_{i,k}(t, \mathcal{P}_1, \mathcal{S}_1) dt + \int_{\tau_1}^{t_2} \sum_{i=1}^{n_F} \sum_{k=1}^K f_{i,k}(t, \mathcal{P}_2, \mathcal{S}_2) dt, \tag{52}
\end{aligned}$$

where (a) is due to the concavity of $f_{i,k}(t, \mathcal{P}, \mathcal{S})$ which was proved in the first part. In other words, for any non-constant resource allocation policy within an epoch, there always exists at least one constant resource allocation policy which achieves at least the same performance. As a result, the optimal resource allocation policy is constant within each epoch. \square

Remark 4: We would like to emphasize that although the fact that the resource allocation policy is constant within each epoch seems obvious in hindsight, it does not necessarily always hold. In the extreme case, when the transformed objective function is strictly convex w.r.t. to the optimization variables, then we can replace “ \geq ” by “ $<$ ” in (52) of the above proof. As a result, there always exists at least one adaptive resource allocation policy which outperforms the constant resource allocation policy.

REFERENCES

- [1] H. Zhu and J. Wang, “Chunk-Based Resource Allocation in OFDMA Systems – Part II: Joint Chunk, Power and Bit Allocation,” *IEEE Trans. Commun.*, vol. 60, pp. 499–509, Feb. 2012.
- [2] K. Seong, M. Mohseni, and J. Cioffi, “Optimal Resource Allocation for OFDMA Downlink Systems,” in *Proc. IEEE Intern. Sympos. on Inform. Theory*, Jul. 2006, pp. 1394–1398.
- [3] Y. Chen, S. Zhang, S. Xu, and G. Li, “Fundamental Trade-offs on Green Wireless Networks,” *IEEE Commun. Mag.*, vol. 49, pp. 30–37, Jun. 2011.
- [4] C. Han, T. Harrold, S. Armour, I. Krikididis, S. Videv, P. Grant, H. Haas, J. Thompson, I. Ku, C.-X. Wang, T. A. Le, M. Nakhai, J. Zhang, and L. Hanzo, “Green Radio: Radio Techniques to Enable Energy-Efficient Wireless Networks,” *IEEE Commun. Mag.*, vol. 49, pp. 46–54, Jun. 2011.

¹²Resource allocation policy $\{\mathcal{P}_3, \mathcal{S}_3\}$ is also a feasible solution to (14) by the convexity of the feasible solution set.

- [5] H. Bogucka and A. Conti, “Degrees of Freedom for Energy Savings in Practical Adaptive Wireless Systems,” *IEEE Commun. Mag.*, vol. 49, pp. 38–45, Jun. 2011.
- [6] G. P. Fettweis and E. Zimmermann, “ICT Energy Consumption - Trends and Challenges,” in *Proc. of the 11th International Symposium on Wireless Personal Multimedia Communications*, Sep. 2008, pp. 1–5.
- [7] C. Li, S. Song, J. Zhang, and K. Letaief, “Maximizing Energy Efficiency in Wireless Networks with a Minimum Average Throughput Requirement,” in *Proc. IEEE Wireless Commun. and Networking Conf.*, Apr. 2012, pp. 1130–1134.
- [8] G. Miao, N. Himayat, and G. Li, “Energy-Efficient Link Adaptation in Frequency-Selective Channels,” *IEEE Trans. Commun.*, vol. 58, pp. 545–554, Feb. 2010.
- [9] G. Miao, N. Himayat, G. Li, and S. Talwar, “Low-Complexity Energy-Efficient Scheduling for Uplink OFDMA,” *IEEE Trans. Commun.*, vol. 60, pp. 112–120, Jan. 2012.
- [10] D. W. K. Ng, E. S. Lo, and R. Schober, “Energy-Efficient Resource Allocation in Multi-Cell OFDMA Systems with Limited Backhaul Capacity,” *IEEE Trans. Wireless Commun.*, vol. 11, pp. 3618–3631, Oct. 2012.
- [11] R. Prabhu and B. Daneshrad, “Energy-Efficient Power Loading for a MIMO-SVD System and Its Performance in Flat Fading,” in *Proc. IEEE Global Telecommun. Conf.*, Dec. 2010, pp. 1–5.
- [12] C. He, B. Sheng, P. Zhu, and X. You, “Energy Efficiency and Spectral Efficiency Tradeoff in Downlink Distributed Antenna Systems,” *IEEE Trans. Wireless Commun. Lett.*, vol. 1, pp. 153–156, Jun. 2012.
- [13] D. Ng, E. Lo, and R. Schober, “Energy-Efficient Resource Allocation in OFDMA Systems with Large Numbers of Base Station Antennas,” *IEEE Trans. Wireless Commun.*, vol. 11, no. 9, pp. 3292–3304, Sep. 2012.
- [14] C. Han, T. Harrold, S. Armour, I. Krikidis, S. Videv, P. Grant, H. Haas, J. Thompson, I. Ku, C.-X. Wang, T. A. Le, M. Nakhai, J. Zhang, and L. Hanzo, “Green Radio: Radio Techniques to Enable Energy-Efficient Wireless Networks,” *IEEE Commun. Mag.*, vol. 49, pp. 46–54, Jun. 2011.
- [15] A. Fehske, P. Marsch, and G. Fettweis, “Bit Per Joule Efficiency of Cooperating Base Stations in Cellular Networks,” in *Proc. Global Telecommun. Conf. Workshops*, Dec. 2010, pp. 1406–1411.
- [16] J. Yang and S. Ulukus, “Optimal Packet Scheduling in an Energy Harvesting Communication System,” *IEEE Trans. Commun.*, vol. 60, pp. 220–230, Jan. 2012.
- [17] C. K. Ho and R. Zhang, “Optimal Energy Allocation for Wireless Communications with Energy Harvesting Constraints,” *IEEE Trans. Signal Process.*, vol. 60, pp. 4808–4818, Sep. 2012.
- [18] K. Tutuncuoglu and A. Yener, “Optimum Transmission Policies for Battery Limited Energy Harvesting Nodes,” *IEEE Trans. Wireless Commun.*, vol. 11, pp. 1180–1189, Mar. 2012.
- [19] O. Ozel, K. Tutuncuoglu, J. Yang, S. Ulukus, and A. Yener, “Transmission with Energy Harvesting Nodes in Fading Wireless Channels: Optimal Policies,” *IEEE J. Sel. Areas Commun.*, vol. 29, pp. 1732–1743, Sep. 2011.
- [20] M. Anteppli, E. Uysal-Biyikoglu, and H. Erkal, “Optimal Packet Scheduling on an Energy Harvesting Broadcast Link,” *IEEE J. Sel. Areas Commun.*, vol. 29, pp. 1721–1731, Sep. 2011.
- [21] O. Ozel, J. Yang, and S. Ulukus, “Optimal Broadcast Scheduling for an Energy Harvesting Rechargeable Transmitter with a Finite Capacity Battery,” *IEEE Trans. Wireless Commun.*, vol. 11, pp. 2193–2203, Jun. 2012.
- [22] J. Yang, O. Ozel, and S. Ulukus, “Broadcasting with an Energy Harvesting Rechargeable Transmitter,” *IEEE Trans. Wireless Commun.*, vol. 11, pp. 571–583, Feb. 2012.
- [23] Huawei Technologies Co., Ltd., “Green Communications, Green Huawei, Green World: Renewable Energy.” [Online]. Available: <http://www.greenhuawei.com/green/greenenergy.html>
- [24] C. Wang and M. Nehrir, “Power Management of a Stand-Alone Wind/Photovoltaic/Fuel Cell Energy System,” *IEEE Trans. on Energy Conversion*, vol. 23, pp. 957–967, Sep. 2008.
- [25] E. Uysal-Biyikoglu and A. El Gamal, “On Adaptive Transmission for Energy Efficiency in Wireless Data Networks,” *IEEE Trans. Inf. Theory*, vol. 50, pp. 3081–3094, Dec. 2004.

- [26] C. Huang, R. Zhang, and S. Cui, "Outage Minimization in Fading Channels Under Energy Harvesting Constraints," in *Proc. IEEE Intern. Commun. Conf.*, Jun. 2012, pp. 5788–5793.
- [27] D. Giancristofaro, "Correlation Model for Shadow Fading in Mobile Radio Channels," *IEE Elec. Lett.*, vol. 32, pp. 958–959, May 1996.
- [28] W. Saad, Z. Han, H. Poor, and T. Basar, "Game-Theoretic Methods for the Smart Grid: An Overview of Microgrid Systems, Demand-Side Management, and Smart Grid Communications," *IEEE Signal Process. Mag.*, vol. 29, pp. 86–105, Sep. 2012.
- [29] M. Tao, Y.-C. Liang, and F. Zhang, "Resource Allocation for Delay Differentiated Traffic in Multiuser OFDM Systems," *IEEE Trans. Wireless Commun.*, vol. 7, pp. 2190–2201, Jun. 2008.
- [30] W. W. L. Ho and Y.-C. Liang, "Optimal Resource Allocation for Multiuser MIMO-OFDM Systems With User Rate Constraints," *IEEE Trans. Veh. Technol.*, vol. 58, pp. 1190–1203, Mar. 2009.
- [31] W. Dinkelbach, "On Nonlinear Fractional Programming," *Management Science*, vol. 13, pp. 492–498, Mar. 1967. [Online]. Available: <http://www.jstor.org/stable/2627691>
- [32] D. W. K. Ng, E. S. Lo, and R. Schober, "Energy-Efficient Resource Allocation for Secure OFDMA Systems," *IEEE Trans. Veh. Technol.*, vol. 61, pp. 2572–2585, Jul. 2012.
- [33] C. Y. Wong, R. S. Cheng, K. B. Letaief, and R. D. Murch, "Multiuser OFDM with Adaptive Subcarrier, Bit, and Power Allocation," *IEEE J. Sel. Areas Commun.*, vol. 17, pp. 1747–1758, Oct. 1999.
- [34] Z.-Q. Luo and S. Zhang, "Dynamic Spectrum Management: Complexity and Duality," *IEEE J. Select. Topics in Signal Process.*, vol. 2, pp. 57–73, Feb. 2008.
- [35] S. Boyd and L. Vandenberghe, *Convex Optimization*. Cambridge University Press, 2004.
- [36] W. Yu and J. M. Cioffi, "FDMA Capacity of Gaussian Multiple-Access Channels with ISI," *IEEE Trans. Commun.*, vol. 50, pp. 102–111, Jan. 2002.
- [37] S. Boyd, L. Xiao, and A. Mutapcic, "Subgradient Methods," *Notes for EE392o Stanford University Autumn, 2003-2004*.
- [38] D. Bertsekas, "Convergence of Discretization Procedures in Dynamic Programming," *IEEE Trans. Automatic Control*, vol. 20, pp. 415–419, Jun. 1975.
- [39] D. P. Bertsekas, *Dynamic Programming and Optimal Control*, 3rd ed. Athena Scientific, 2006.
- [40] P. Nuggehalli, V. Srinivasan, and R. Rao, "Energy Efficient Transmission Scheduling for Delay Constrained Wireless Networks," *IEEE Trans. Wireless Commun.*, vol. 5, pp. 531–539, Mar. 2006.
- [41] S. Schaible, "Fractional Programming. II, On Dinkelbach's Algorithm," *Management Science*, vol. 22, pp. 868–873, 1976. [Online]. Available: <http://www.jstor.org/stable/2630018>
- [42] "3rd Generation Partnership Project; Technical Specification Group Radio Access Network; Evolved Universal Terrestrial Radio Access (E-UTRA); Further Advancements for E-UTRA Physical Layer Aspects (Release 9)," 3GPP TR 36.814 V9.0.0 (2010-03), Tech. Rep.
- [43] M. Ergen, *Mobile Broadband: Including WiMAX and LTE*, 1st ed. Springer, 2009.
- [44] R. Kumar and J. Gurugubelli, "How Green the LTE Technology Can be?" in *Intern. Conf. on Wireless Commun., Veh. Techn., Inform. Theory and Aerosp. Electron. Syst. Techn.*, Mar. 2011.
- [45] D. Tse and P. Viswanath, *Fundamentals of Wireless Communication*, 1st ed. Cambridge University Press, 2005.